2007-08-21

Development of a New Ca II H and K Spectrophotometric Temperature Index

Kathleen Elizabeth Moncrieff
Brigham Young University - Provo

DEVELOPMENT OF A NEW CALCIUM II H AND K SPECTROPHOTOMETRIC TEMPERATURE INDEX

by

Kathleen Elizabeth Moncrieff

A thesis submitted to the faculty of

Brigham Young University

in partial fulfillment of the requirements for the degree of

Master of Science

Department of Physics and Astronomy

Brigham Young University

December 2007

BRIGHAM YOUNG UNIVERSITY

GRADUATE COMMITTEE APPROVAL

of a thesis submitted by

Kathleen Elizabeth Moncrieff

This thesis has been read by each member of the following graduate committee and by majority vote has been found to be satisfactory.

Date	Eric G. Hintz, Chair
Date	Benjamin J. Taylor
Date	Michael D. Joner
Date	J. Ward Moody

BRIGHAM YOUNG UNIVERSITY

As chair of the candidate's graduate committee, I have read the thesis of Kathleen Elizabeth Moncrieff in its final form and have found that (1) its format, citations, and bibliographical style are consistent and acceptable and fulfill university and department style requirements; (2) its illustrative materials including figures, tables, and charts are in place; and (3) the final manuscript is satisfactory to the graduate committee and is ready for submission to the university library.

Date

Eric G. Hintz
Chair, Graduate Committee

Accepted for the Department

J. Ward Moody, Graduate Coordinator
Department of Physics and Astronomy

Accepted for the College

Tom W. Sederberg, Associate Dean
College of Physical and Mathematical Sciences

ABSTRACT

DEVELOPMENT OF A NEW CALCIUM II H AND K

SPECTROPHOTOMETRIC TEMPERATURE INDEX

Kathleen Elizabeth Moncrieff

Department of Physics and Astronomy

Master of Science

We are developing a new spectrophotometric temperature index based on the Ca II H and K lines. Because these lines are present even in very cool stars and because the Ca II H line is blended with the Hϵ line in hot stars, this index should cover a very broad range of spectral types. Our data set consisted of 95 stars with spectral types ranging from O9 to M1. We examined five different indices based on the Ca II H + Hϵ and K lines, as well as single-wavelength indices centered on each of the Hδ and Hγ lines, which are in the same region of the spectrum. We compared our new index value with the Hβ index values for the stars in our data set that had published Hβ values. We found that the Ca II K-H index was the best temperature indicator with the widest range in magnitude of the indices we examined.

ACKNOWLEDGMENTS

First, I would like to thank my advisor, Dr. Hintz, and my other committee members, Prof. Joner, Dr. Taylor, and Dr. Moody, for all of their help and support and for editing my many drafts, as well as Maureen Hintz and Lisa Joner for their help with editing. I would also like to thank Tabitha Bush and Liberty Evanko for their help with IRAF, general astronomy questions, and other things. Thanks to Jake Albretson for help with computer stuff and for putting Linux on the computer in my office, and to Ben Rose for help with LaTex issues. And I would like to thank Diann Sorensen, our amazing graduate secretary, for the countless hours that she has spent helping me with paperwork and other things. Finally, I would like to thank my parents, as well as James Moncrieff and Kelly Blackmore, for all of their support and encouragement.

Contents

List of Tables

List of Figures

Chapter 1

Introduction and Background

1.1 Introduction

How do we know the temperatures of stars? We obviously can't go visit a star and stick a thermometer in it. The only information we have about stars comes in the form of a tiny point of light in the sky. But by analyzing these points of light, we can find incredible amounts of information about many different properties of stars. By splitting the light into its component wavelengths, we can see which absorption and emission lines are found in the star, and how strong those spectral features are.

The Boltzmann and Saha equations make it possible for us to determine ratios of populations of different excitation or ionization levels for different elements as a function of temperature. Because of this, measuring the relative strengths of different absorption lines in the spectrum of a star can help us find the temperature of the star, which is directly related to its spectral type.

There have been several spectral indices developed for stars using hydrogen lines, such as the Hβ index. In this project, we will examine several new spectral index based on the Ca II H and K lines as well as the Hδ and Hγ lines, which are in the same spectral region, using synthetic filter functions. The Ca II H line has a wavelength of 3969 Å and the Ca II K line has a wavelength of 3934 Å. Cooler stars, however, do not have strong hydrogen lines, and so these indices do not work as well for later spectral types. The Ca II H line is blended with Hϵ (at 3970 Å) in hotter stars. Figure 1.1 shows this region of the spectrum for stars of 4 different spectral types. Ca II H and K lines are present in stars of spectral type A through M, so an index based on the Ca II lines will cover a broader range of spectral types than an index based on hydrogen lines. Another advantage is that the two lines are

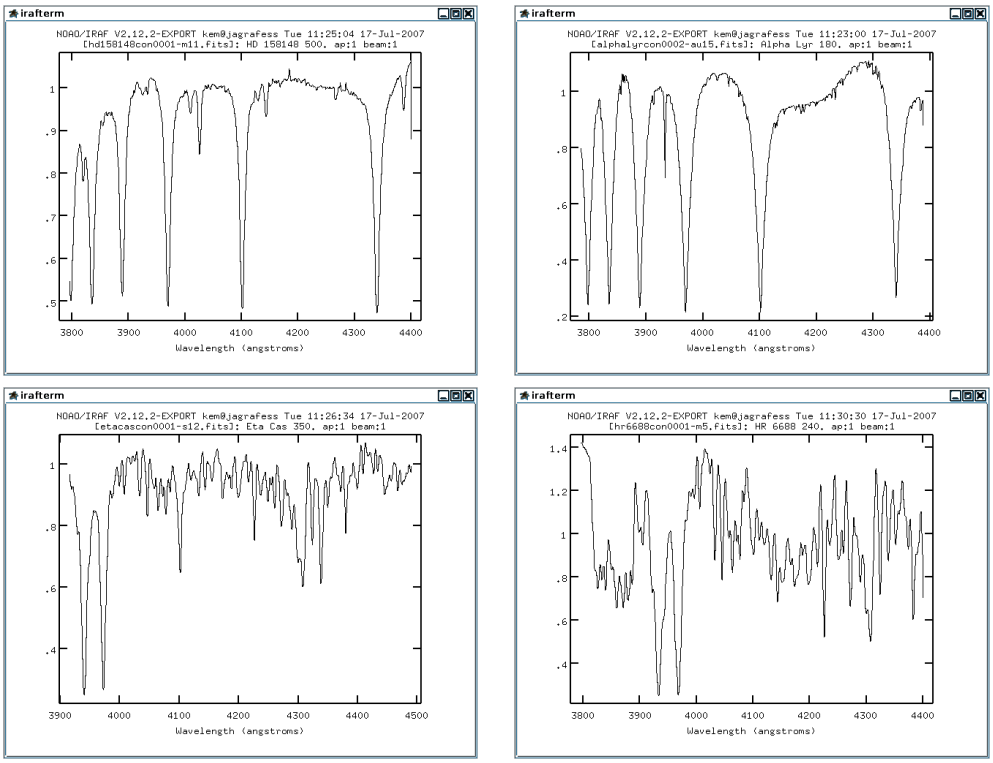

Figure 1.1: The Ca II H and K lines in stars of four different spectral types. In the star at the top left, a B5 star, we only see the Hϵ line. In the star at the top right, an A0 star, we can see the Hϵ line blended with the Ca II H line, and we start to see the Ca II K line. In the star at the bottom left, a G0 star, we see strong Ca II H and K lines, but we can still see the Hδ and Hγ lines to the right of the Ca II lines. In the star at the bottom right, a K2 star, we see strong Ca II lines but no hydrogen lines.

fairly close in wavelength, and so they should not be greatly affected by differential interstellar reddening (see Section 1.6).

We will show in this study that the Ca II lines can be used to form a spectral index by comparing this new spectral index with the Hβ index. We will examine several different forms that the index could take. We will also discuss the effects of metallicity on the index.

1.2 Astronomical Magnitudes

We classify stars using the magnitude scale, which is quantified by the equation

$$M = -2.5logF + zeropoint \tag{1.1}$$

where M is the magnitude, F is the flux, and the zero point is just an arbitrary zero point. Often a number that is simply much lower than the magnitudes of the stars in question is chosen, or the stars are compared to a standard star or group of stars. The apparent magnitude (the magnitude that we observe, not taking into consideration the fact that stars are all at different distances from us) of a star is related to its apparent luminosity. The absolute magnitude (the magnitude that we would observe if all stars were at a set distance from us) is related to the star's intrinsic or absolute luminosity.

The magnitude system was created by the ancient Greek astronomer Hipparchus. He classified all of the stars he could see on a logarithmic scale using the numbers one through six, with one referring to the brightest stars and six to the faintest. The current magnitude scale still has magnitude values increasing as stars get fainter and decreasing as stars get brighter.

1.3 The H-R Diagram

A Hertzsprung-Russell diagram, or H-R diagram, is a plot of absolute magnitude or luminosity vs. spectral type or temperature (all of these plots are equivalent) for a group of stars. An example of an H-R diagram is shown in Figure 1.2.

Spectral types were first assigned to stars according to the strengths of their hydrogen Balmer lines. Different letters of the alphabet were assigned to the different spectral types with "A" meaning strong absorption and subsequent letters indicating weaker absorption. The sequence of spectral types was later rearranged in order of temperature, and the types were subdivided using the numbers 0-9. The sequence of spectral types we use now is OBAGKFM, which is arranged in order of decreasing

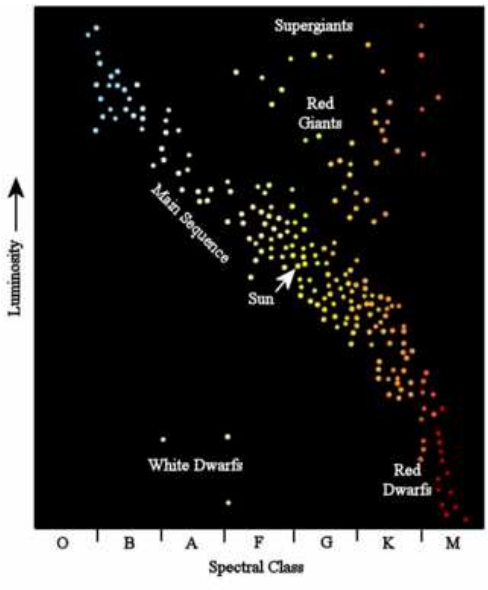

Figure 1.2: An example of an H-R diagram. Spectral type is plotted on the x-axis, and luminosity is on the y-axis. Image from http://commons.wikimedia.org/wiki/Image:HR-sparse.svg

temperature. A plot of magnitude vs. a particular color, or a color-magnitude diagram, is very similar to an H-R diagram. Color in this sense refers to the difference in magnitude of an object when measured in different filters. As stars evolve, they move across the H-R diagram in certain paths dictated by their initial masses and compositions, as their characteristics like temperature, spectral type, and luminosity change. Having accurate ways of determining stars' spectral types and temperatures, coupled with information about the stars' sizes and compositions, gives us information about what stages stars are at in their evolution.

1.4 Spectral Types

Stars are classified into spectral types based on the strengths of various spectral lines. Since stars' temperatures are related to the strengths of their hydrogen lines, relative hydrogen line strengths can be used to make temperature indices. Figure 1.3 shows what the spectra of stars of several different spectral types look like.

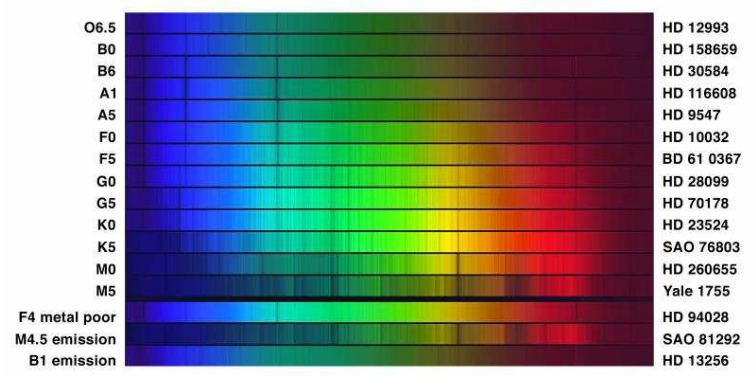

Figure 1.3: Examples of spectra for stars of various spectral types and metallicities. Image from http://antwrp.gsfc.nasa.gov/apod/ap040418.html

1.5 Temperature Measurements

We can get a general idea of a star's temperature (and subsequently its spectral type) by looking at its color. Cooler stars are redder, while hotter stars are bluer. This is because stars are well approximated by blackbodies. Blackbodies emit light at a peak wavelength which depends solely on their temperature,

$$\lambda_{max} = 2.898 \times 10^7 T, \tag{1.2}$$

where T is the temperature in Kelvin and λ_{max} is the peak wavelength in Å. We see from this that the higher the temperature of the blackbody, the lower the peak wavelength. The equation

$$I(\lambda, T) = \frac{2hc^2}{\lambda^5} \frac{1}{e^{\frac{hc}{\lambda kT}} - 1}, \tag{1.3}$$

where I(λ,T) is the intensity as a function of wavelength and temperature, gives the shape of the curve. This is also called the Planck function, and we can plot it as a function of temperature for a given wavelength to find what the blackbody curve

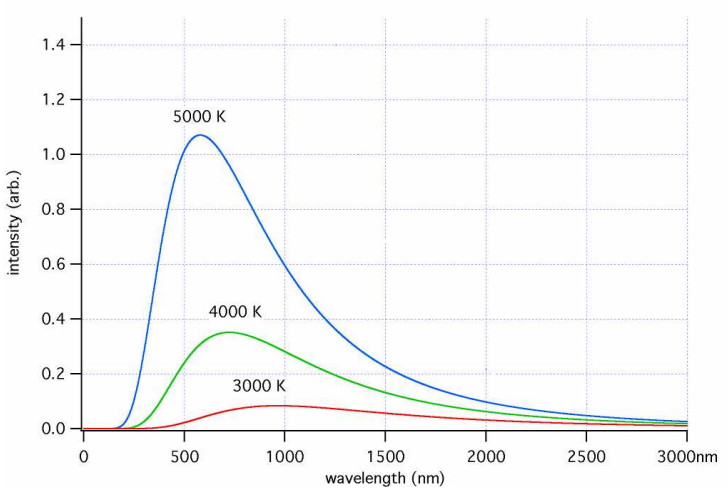

Figure 1.4: Examples of blackbody curves for objects of three different temperatures. Image from http://commons.wikimedia.org/wiki/Image:Blackbody-lg.png

of an object of a given temperature looks like. Figure 1.4 shows qualitatively what blackbody curves look like for objects of three different temperatures.

Another way to measure the temperatures of stars is by looking at their spectra and measuring the relative strengths of different spectral lines. The atomic and molecular transitions that correspond to lines at specific wavelengths are well established and easy to determine. Measuring the relative strengths of different absorption or emission lines gives us an idea of the relative numbers of particles undergoing those transitions. The Saha equation gives us the ratio of the number densities of particles in different ionization states and the Boltzmann equation gives us the ratio of the number densities of particles in different excitation states. Both of these equations depend on temperature, which means that the ratios of the strengths of different spectral features vary as a function of temperature. Although in this project we will not be calculating exact temperatures of stars using any of these equations, this serves as the theoretical motivation that allows us to use the colors of stars and the relative

Table 1.1. Values of A_λ for our filters

Filter	Central Wavelength (Å)	A_λ
Ca II K	3934	0.0460
Ca II H	3969	0.0457
Ca II H and K	3960	0.0458
Hδ	4101	0.0444
Hγ	4340	0.0418

strengths of different spectral features for comparing the temperatures of stars and creating spectral indices.

1.6 Interstellar Reddening

Starlight travels through quite a bit of dust before we observe it. There are about $5x10^{26}$ dust particles between us and the nearest star (Laverty 2006). Dust scatters blue light more than red light, making light from distant objects appear redder than it actually was when it left the object. Since stars are essentially blackbodies, their temperatures are directly related to their colors. Hotter stars are bluer and cooler stars are redder. If the light appears redder than it actually is, the temperature we measure is lower than the object's actual temperature. Because of this effect, reddening is one of the main problems we encounter when we try to measure stellar temperatures. Shorter wavelengths are affected by interstellar reddening to a greater extent than longer wavelengths are, so when we use color indices that are not based on a single wavelength, we can potentially measure inaccurate temperatures. Because the Ca II H and K lines are so close together in wavelength, however, the effects of reddening in this case should not cause significant errors for nearby stars, and reddening effects were not considered in this study. Table 1.1 list values of A_λ for the central wavelengths of the filters used, calculated using the method outlined in Cardelli et al. (1989).

1.7 Photometry and Temperature Indices

There are a variety of different temperature indices that have been established for stars, but all of these indices fall into two main categories - single wavelength indices and multiple wavelength indices. Multiple wavelength indices are formed by obtaining magnitudes in two different wavelength ranges (usually photometrically with the use of different colored filters, such as B-V or V-R) and subtracting them. Single wavelength indices are made by obtaining magnitudes in a wide filter and a narrow filter centered on the same wavelength and subtracting them. Single wavelength indices have the advantage of not being affected by reddening, since the filters have the same central wavelength and reddening is wavelength dependent. Photometric indices are formed with data from photometric observations. In this study, we are examining spectrophotometric indices. Spectrophotometry involves using synthetic filter functions to find magnitude from spectroscopic data.

1.8 The Hydrogen Balmer Lines

The hydrogen Balmer series results from electron transitions between the n=2 state and higher states. They are strongest in B-G stars, and are very weak in cool K and M stars and hot O stars. Three of the Balmer lines are found in the spectral region involved in this study: Hγ, Hδ, and Hϵ. As previously stated, the Hϵ line is located at 3970 Å and is blended with Ca II H in hotter stars (spectral type greater than about A0). The Hγ and Hδ lines are located at 4340 Å and 4101 Å, respectively.

1.9 The Ca II H and K Lines

As previously mentioned, the Ca II H and K lines are located at 3969 Å and 3934 Å, respectively. These lines result from a doublet transition from the ground state of singly ionized calcium to the first excited state, shown in Figure 1.5. The unsaturated ratio of Ca II K to Ca II H in absorption features is 2 to 1, which is typical for S-P doublet lines in sodium-like ions.

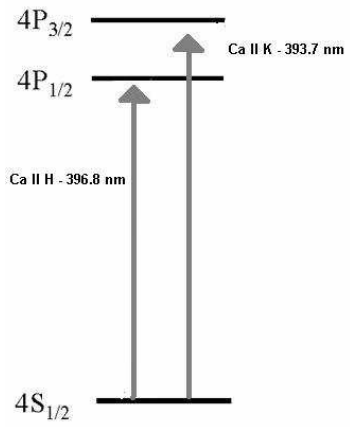

Figure 1.5: Energy level diagram of the transitions that cause the Ca II H and K absorption lines. This is a doublet transition from the ground state to the first excited state of singly ionized calcium.

1.9.1 Discovery and Properties of the Ca II H and K Lines in the Solar Spectrum

The Ca II H and K lines were observed as absorption lines in the spectrum of the Sun in 1814 by Joseph von Fraunhofer. Fraunhofer catalogued and measured the wavelengths of hundreds of dark lines that are visible in the Sun's spectrum. The strongest lines were designated with the letters A through K, omitting I and J. Thus the lines H and K were right next to each other. These lines were later identified with Ca II, as discussed in the preceding section.

In the Sun, Ca II H and K emission lines are observed in the lower chromosphere, in spicules, and in solar prominences. Regions with high magnetic fields seem to coincide with regions of high Ca II H and K emission. Ca II H and K emission also appears to be related to supergranulation. The Ca II H and K lines are the main source of information about chromospheric structure in the Sun. (Linsky & Avrett 1970).

1.9.2 Some Basic Properties of the Ca II H and K Lines in Stars

It has been known for some time that the Ca II H and K lines in stars are related to metallicity and chromospheric activity. Several interesting features of the H and K lines in stars are noted in Linsky & Avrett (1970):

1. In stars of spectral type later than G0, the width of emission in the cores of these lines increases linearly as absolute magnitude increases. This is called the Wilson-Bappu effect.

2. The ratio of the strength of the K line to the H line increases with chromospheric activity.

3. In long period M variables, the H and K lines are broad absorption features near the stars' maximum light and then they turn into narrow emission features near the stars' minimum light.

4. In T Tauri stars, the H and K lines are often seen as broad emission features that can be ten times as bright as the continuum.

1.10 Previous Work in Ca II H and K Photometry

Several astronomers over the past few decades have used the Ca II H and K lines to create different indices for stars. Zinn (1980) used a photometric filter based on the Ca II H and K lines in conjunction with several other filters to construct a composite reddening-free photometric index for stars in globular clusters. Suntzeff (1980) constructed a spectroscopic index that compared the strength of the combined H and K lines to the continuum on either side of the lines. He found these values to be well correlated with metallicity for giant stars in globular clusters. Beers et al. (1985) created a spectroscopic index centered on just the Ca II K line that compared that line strength to the continuum on either side. This avoided the issue of Hϵ being blended with the Ca II H line in hotter stars, which tends to make that line less

sensitive to metallicity in hotter stars. They found that this was a good indicator of metallicity in stars with [Fe/H]<-2.

Anthony-Twarog et al. (1991) decided to create a photometric index using these lines. This index is a good metal indicator, especially for metal-poor dwarfs and red giants because the Ca II lines are strong even in metal-poor stars. They chose to use a narrow band filter in order to get around what they say is the main problem with photometry, low resolution. Their filter, called Ca, is 90 Å wide, centered at 3960 Å and covers both lines. This makes it 1/2 to 1/4 the wavelength width of the other filters in the uvby system. Their index is defined as $hk = (Ca - b) - (b - y)$. In the 1991 paper they list index values for 163 standard stars. In a second paper in 1995, they present a catalog of 1990 stars of spectral type B-M, luminosity class I-VI, and [Fe/H] from above solar values to -4.5 (Anthony-Twarog et al. 1995). In a third paper in 1998, they present values for about 300 more stars and discuss reddening corrections (Anthony-Twarog & Twarog 1998). Hintz et al. (1998) used Caby photometry to find [Fe/H] values for δ Scuti variables.

1.11 Advantages of a Spectral Index Using the Ca II H and K Lines

One of the main advantages of using these two lines as the basis for a spectral index is that they are present in a wide range of spectral types. They are present in very cool K and M stars, where the hydrogen Balmer lines, which are commonly used to make spectral indices, are not present. In hot O and B stars, where the Ca II H and K lines disappear, the Ca II H line is blended with the H epsilon line, so an index centered at the Ca II H and K wavelengths will still be able to measure something in hot stars. This means that this index should work for essentially all spectral types. The other main advantage of this index is that the Ca II lines are very close together, which means that the effects of interstellar reddening should be small, at least for stars that are not highly reddened and for observations taken at low airmasses.

Chapter 2

Procedures

2.1 Observations

Our spectroscopic observations were taken with the 1.2-m telescope at the Dominion Astrophysical Observatory in September 2003, April 2004, August 2004, and May 2005. Appendix A lists the stars in our data set. Exposure times ranged from 30-900 seconds depending on atmospheric conditions and the magnitude of the star. Our dispersion was around 0.15 Å per pixel.

2.1.1 Calibration Frames

Three types of calibration frames were taken for these observations. Zero frames (also called bias frames) were taken to correct for pixel to pixel variation in charge across the CCDs. Flat field frames were taken to correct for variation across the CCDs in response to a uniform field of light. Comparison frames (called arcs) were used to wavelength calibrate the spectra. These are images of an iron/argon or thorium/argon arc lamp with lines at known wavelengths in the same wavelength region as our object spectra.

2.2 Data Reduction

Our images were reduced using the Image Reduction and Analysis Facility (IRAF). This section presents an outline of the procedure used to calibrate spectroscopic data.

1. Update image headers - There are certain pieces of information that must be present in the image file headers in order for the other reduction steps to work properly. All frames need to contain the image type information: zero, flat,

comp (for comparison), or object. They should also contain the date and starting time for the observation, an observatory identification keyword, the dispersion axis, the sidereal time, and the exposure time. Object and arc spectra also need some additional information. Object spectra should have the right ascension and declination of the object as well as its name. Objects and arcs both need to have the Julian date and the airmass of the observation added to their headers. These are calculated by IRAF using the date, time, and longitude of the observatory. Most of this information can be added to the headers using the IRAF's *ASTHEDIT* package. Examples of .cmds files are shown in Figure 2.1. The airmass is calculated using the *SETAIRMASS* package, and the Julian date is calculated using the *SETJD* package.

2. Trim images - Most CCDs have bad columns or regions that do not contain actual image information. These regions were removed from our spectra using IRAF's *CCDPROC* package. We removed columns 1-39 and 4001-4200.

3. Remove cosmic rays from images - Cosmic ray hits become a significant concern when dealing with the long exposure times required for spectroscopy, but they are fairly easy to remove. The IRAF package *COSMICRAYS* was used to remove small cosmic ray hits. Larger cosmic rays (which the *COSMICRAYS* package often misinterprets as actual spectral features) were removed by hand.

4. Zero correct images - Our zero frames were averaged together using the package *ZEROCOMBINE* and then subtracted from the flat, arc, and object frames using the *CCDPROC* package. Figure 2.2 shows a combined zero spectrum.

5. Flat field correct images - The zero corrected flat field frames were averaged together using the *FLATCOMBINE* package, and then normalized to an average value of 1 using the *APFLATTEN* package. Since the entire CCD is not exposed to light when taking flats, the edges of the flat field images contain a

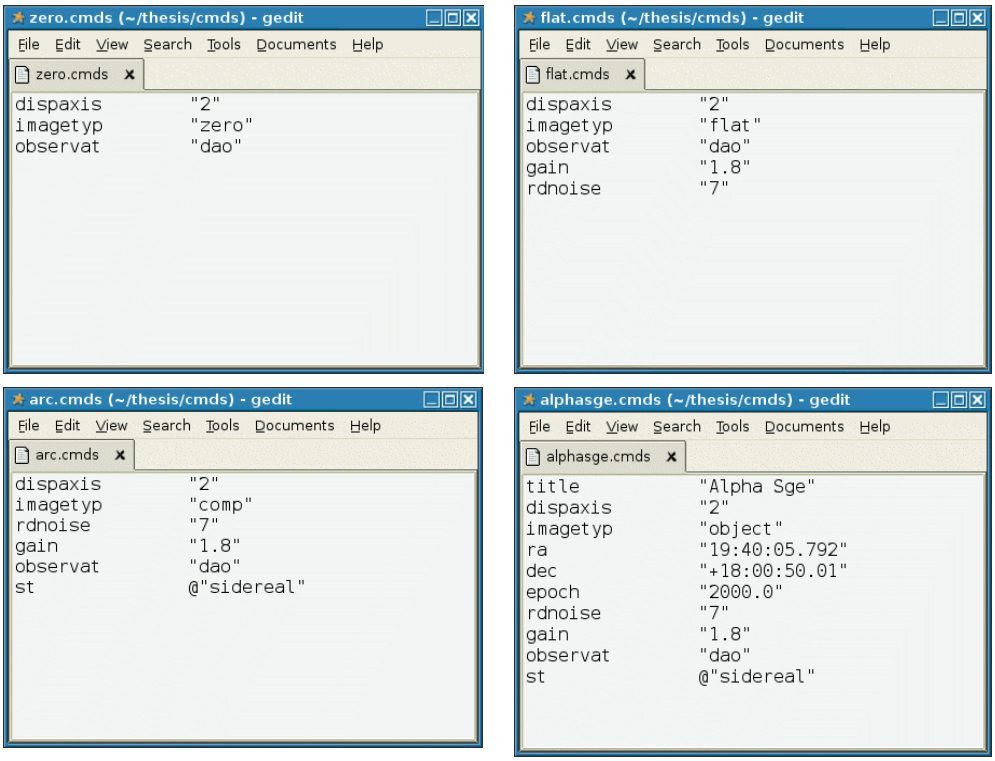

Figure 2.1: Examples of .cmds files. The top left .cmds file is used for zero frames. The top right .cmds file is used for flat field frames. These two .cmds files just contain the dispersion axis, the image type, and the observatory identification. The bottom left file is used for arcs, and the bottom right file is used for objects.

lot of noise and no signal. The *APFLATTEN* package allows the user to select the aperture that contains actual information, which means that the object spectra are only divided by the part of the flats that contains actual information, producing much better results than simply dividing the object spectra by the entire flat field image. Figure 2.3 shows the aperture selection process in *APFLATTEN*. The *CCDPROC* package was then used to remove the flat field variations from the arc and object frames. Figure 2.4 shows combined flat field spectra before and after using *APFLATTEN*. Figure 2.5 shows object spectra before and after the flats and zeros have been applied.

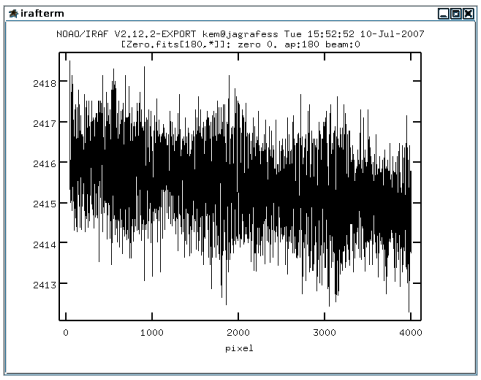

Figure 2.2: A combined zero spectrum.

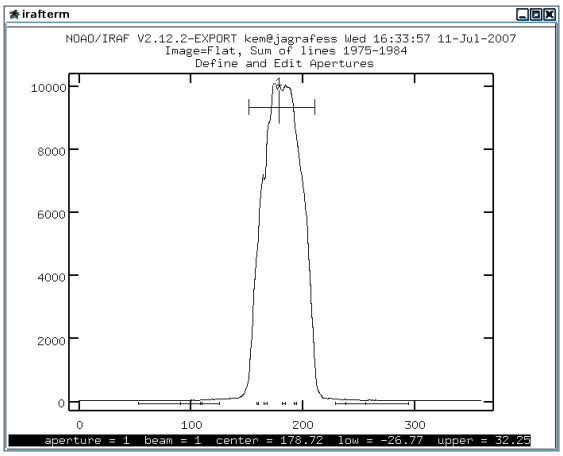

Figure 2.3: A screen shot of the aperture selection process in *APFLATTEN*.

6. Wavelength calibrate image spectra - Our spectra were wavelength calibrated using the IRAF package *DOSLIT*. The *DOSLIT* package combines the tasks of finding apertures for the object spectra, making the two-dimensional spectra into one-dimensional spectra, identifying lines in the arcs, and wavelength calibrating the spectra. Figure 2.6 shows an arc spectrum and an object spectrum that have been wavelength calibrated. Iron/argon arcs were used for the observations from September 2003, August 2004, and May 2005. Thorium/argon arcs were used for the observations from April 2004.

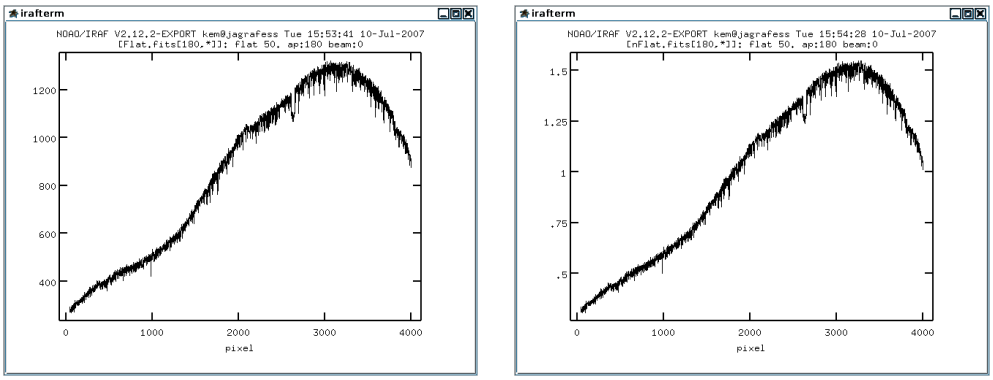

Figure 2.4: Combined flat field spectra. The image on the left has not been normalized; the one on the right has.

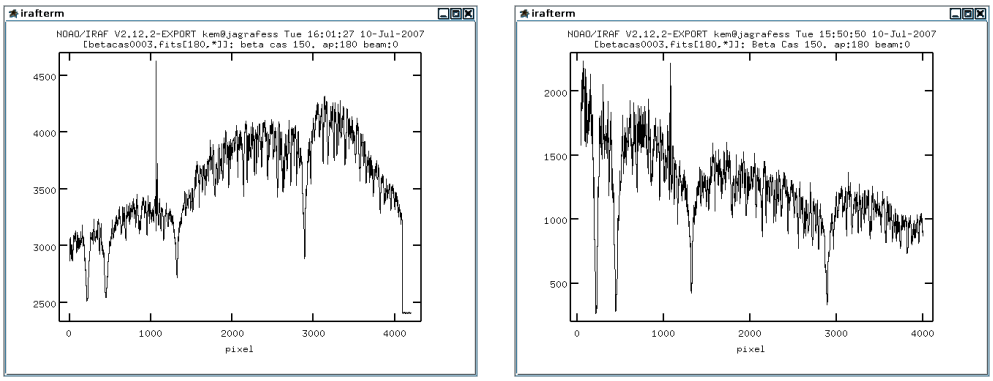

Figure 2.5: Object spectra before and after processing. The image on the right is the same spectrum as the image on the left, but it has been trimmed and had the zeros and flats applied to it.

7. Continuum calibrate image spectra - After wavelength calibration, we used the IRAF package *CONTINUUM* to continuum calibrate the spectra. These were saved as new files so that we could make measurements with both the continuum calibrated and non-continuum calibrated spectra. Figure 2.7 shows a continuum calibrated object spectrum.

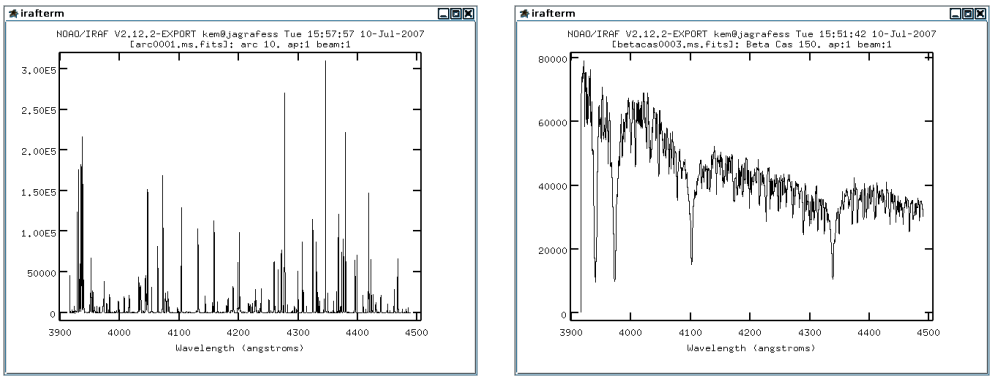

Figure 2.6: Wavelength calibrated spectra. The spectrum on the left is an arc; the spectrum on the right is an object. The spikes in the spectra are cosmic ray hits.

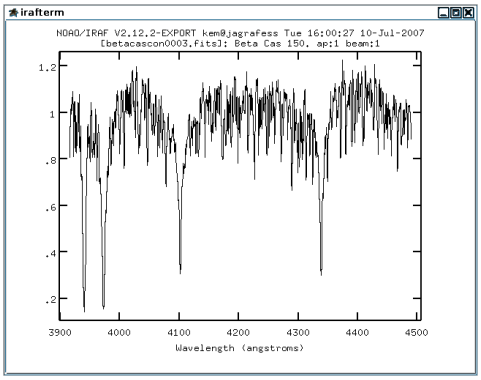

Figure 2.7: A continuum calibrated object spectrum.

2.3 SBANDS

The IRAF package *SBANDS* takes a user-defined filter function and measures the magnitude that would be found if a spectrum were observed through that filter. The user inputs a file (called a bandpass file) that contains the central wavelength, width of the filter, and filename of a filter function file. If no filter function filename is specified, *SBANDS* assumes that the filter response is 1 across the entire width of the filter, essentially creating a square filter. The filter function file is a two column text file with wavelengths in the first column and filter responses at those wavelengths in the second column. This allows the user to create basically any kind of filter, and

also to input traces of actual filters. We chose to use square and Gaussian filters since real filters are almost always somewhere between these two idealized functions. Our filters were defined as follows:

1. 30 angstrom wide filter centered on Ca II K (3934 Å)
2. 30 angstrom wide filter centered on Ca II H (3969 Å)
3. 90 angstrom wide filter centered between Ca II H and K (3960 Å)
4. 30 angstrom wide filter centered on Hγ (4340 Å)
5. 90 angstrom wide filter centered on Hγ (4340 Å)
6. 30 angstrom wide filter centered on Hδ (4101 Å)
7. 90 angstrom wide filter centered on Hδ (4101 Å)

The following Figures show examples of the files involved in using *SBANDS*. Figure 2.8 shows the user created bandpass file that *SBANDS* uses as input. Finally, Figure 2.9 shows part of an output file from *SBANDS*. Finally, Figures 2.10 through 2.12 show graphically the square and Gaussian filter functions that we used.

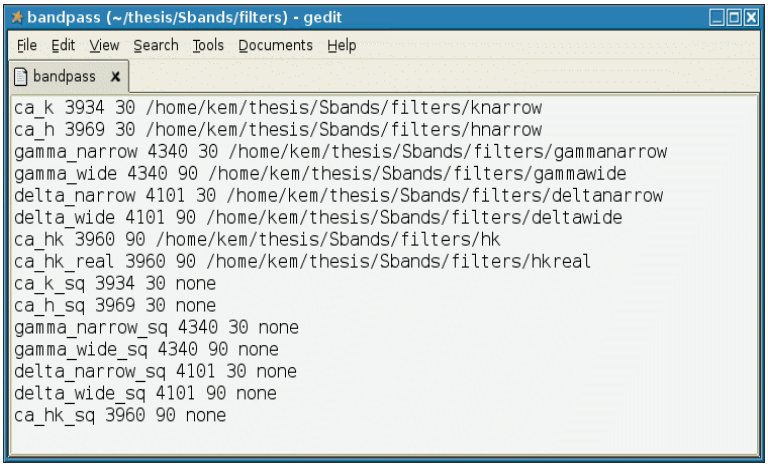

Figure 2.8: An example of an *SBANDS* bandpass file.

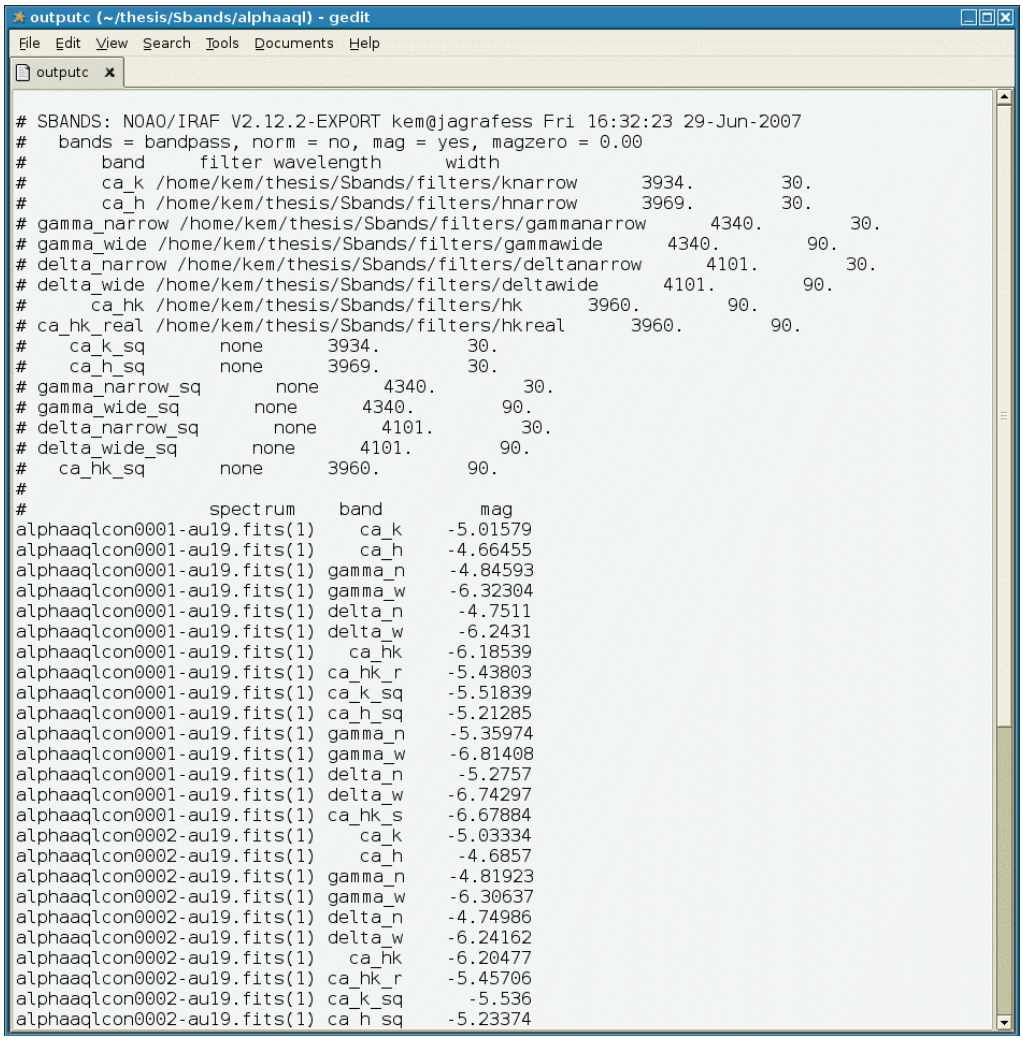

Figure 2.9: An example of part of an *SBANDS* output file.

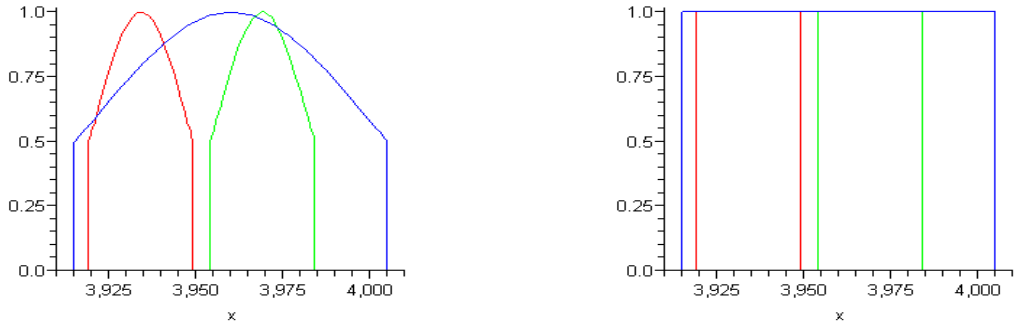

Figure 2.10: The three Ca II H and K filters. The graph on the right shows the Gaussian filter functions; the graph on the left shows the square filter functions. Wavelength in Å is on the x axes and relative filter response is on the y axes.

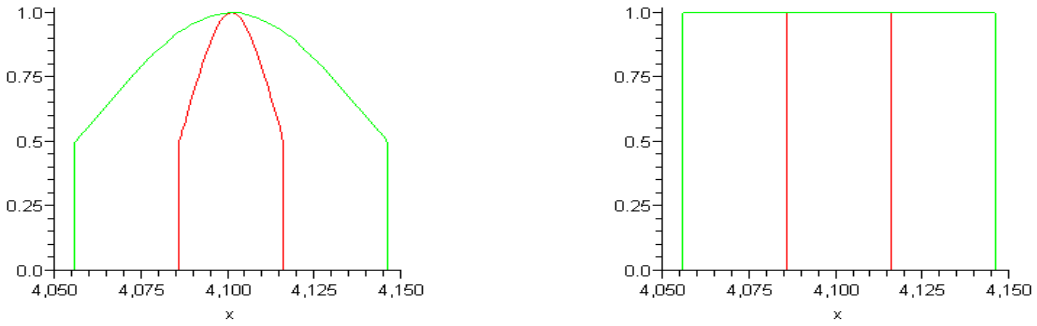

Figure 2.11: The two Hδ filters. The graph on the right shows the Gaussian filter functions; the graph on the left shows the square filter functions. Wavelength in Å is on the x axes and relative filter response is on the y axes.

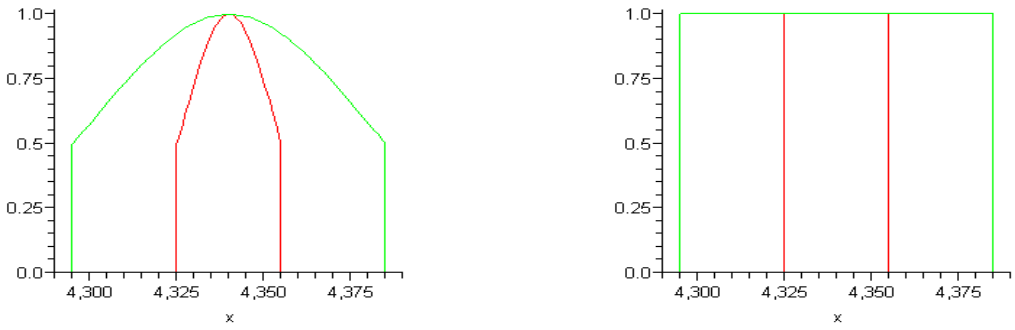

Figure 2.12: The two Hγ filters. The graph on the right shows the Gaussian filter functions; the graph on the left shows the square filter functions. Wavelength in Å is on the x axes and relative filter response is on the y axes.

Chapter 3

Results and Analysis

We examined seven different spectral indices, which are outlined in Table 3.1. The index values were found from magnitudes obtained in $SBANDS$ with synthetic filter functions that we defined, as listed in the previous chapter. We used Gaussian and square filters, and we obtained magnitude values from both continuum calibrated spectra and non-continuum calibrated spectra. We will refer to spectra that have been wavelength calibrated and not continuum calibrated as "wavelength calibrated spectra", and we will refer to spectra that have been both wavelength and continuum calibrated as simply "continuum calibrated spectra". Thus we have four different versions of each index. We plotted these indices versus spectral type for all stars and temperature for the stars in our data set with known temperatures. We also plotted the index values (for all of the indices involving the Ca II lines) versus metallicity for stars with known metallicities to see how that affected our indices. Finally, we compared our index values with published Hβ values for the stars for which that information was available, and we plotted our indices against each other. The rest of this chapter will present and discuss those relations.

3.1 The Hβ Index

The seven spectral indices included in this study were all plotted against published Hβ index values found in the SIMBAD database (2007). Figures 3.1 and 3.2 show Hβ values vs spectral type for the stars in our study with published Hβ values as well as Hβ vs temperature for the stars with both published Hβ values and temperatures. We can see in these plots that Hβ is a good temperature and spectral type indicator for stars of spectral type B-G.

Table 3.1. Spectral indices used in this study

Index Name	Filters Used (Defined in Section 2.3)
Ca II K-H	Filter 1 - Filter 2
Ca II HK-K	Filter 3 - Filter 1
Ca II HK-H	Filter 3 - Filter 2
Hδ	Filter 4 - Filter 5
Hγ	Filter 6 - Filter 7
Ca II (K-H) - Hδ	[Filter 1 - Filter 2] - [Filter 4 - Filter 5]
Ca II K-H) - Hγ	[Filter 1 - Filter 2] - [Filter 6 - Filter 7]

The Hβ index is described in Crawford & Mander (1966). It is a photometric index that uses wide and narrow filters which have the Hβ line as their central wavelength. The index value is defined as the magnitude of the star through the narrow filter minus the magnitude of the star through the wide filter.

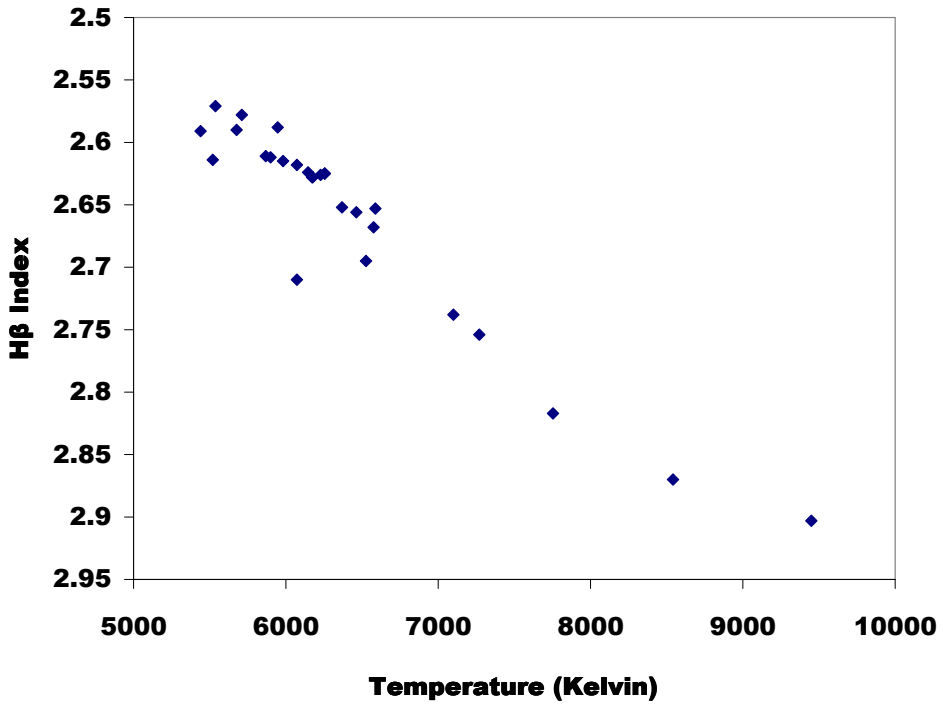

Figure 3.1: Published Hβ values vs spectral type for some of the stars in our study.

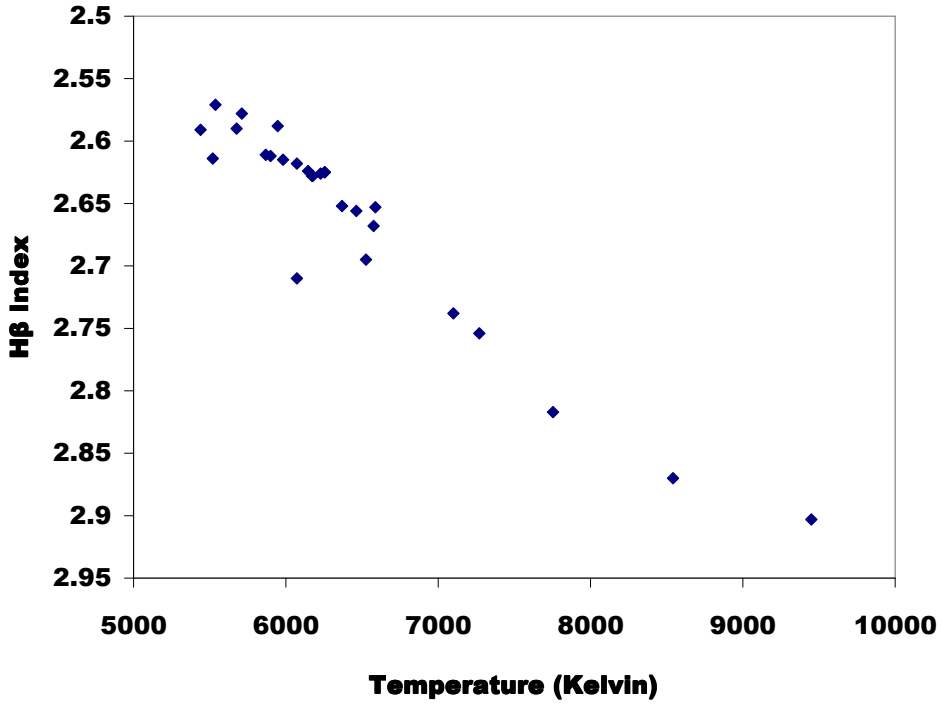

Figure 3.2: Published Hβ values vs temperature for some of the stars in our study.

3.2 The Ca II K-H Index

We define the Ca II K-H index as the magnitude through the narrow filter centered on the Ca II K line minus the magnitude through the narrow filter centered on the Ca II H line. Figure 3.3 shows the Ca II K-H index vs spectral type. In all versions of the index there is a sharp peak around A0. There does not appear to be a significant difference in the range of index values for the Gaussian filters and the square filters, although there appears to be a slight zeropoint offset. There is, however, a difference in the size of the range of values for the continuum calibrated spectra and the wavelength calibrated spectra, with the range for the wavelength calibrated spectra being larger than the range for the continuum calibrated spectra.

Figure 3.4 shows the Ca II K-H index vs temperature. The index appears to lose some sensitivity for the hottest stars and the coolest stars, which is not unexpected. In hot O stars and early B stars, the Hϵ line is essentially gone, and in cool M stars, the two Ca II lines are nearly equal in strength, so at the very edges of the spectral type sequence the Ca II K-H index is probably not a good temperature index. However, there appears to be a correlation with temperature for early B stars through late K stars. There is some scatter in the index values, and there appears to be more scatter in the continuum calibrated spectra than in the wavelength calibrated spectra.

For the spectral type plots, the index values for the continuum calibrated spectra and Gaussian filters have a magnitude range of about 1.0. The index values for the continuum calibrated spectra and square filters have a magnitude range of about 0.8. The values for the the wavelength calibrated spectra and Gaussian filters have a range of about 1.3, and the values for the wavelength calibrated spectra and square filters have a magnitude range of about 1.1. For the temperature plots, the continuum calibrated spectra and Gaussian filters have a magnitude range of about 0.9 and the continuum calibrated spectra and square filters have a range of about 0.8. The wavelength calibrated spectra and Gaussian filters have a range of about 1.1,

and the wavelength calibrated spectra and square filters have a range of about 1.0. In both the spectral type plots and the temperature plots, the wavelength calibrated spectra and Gaussian filters have the widest magnitude range.

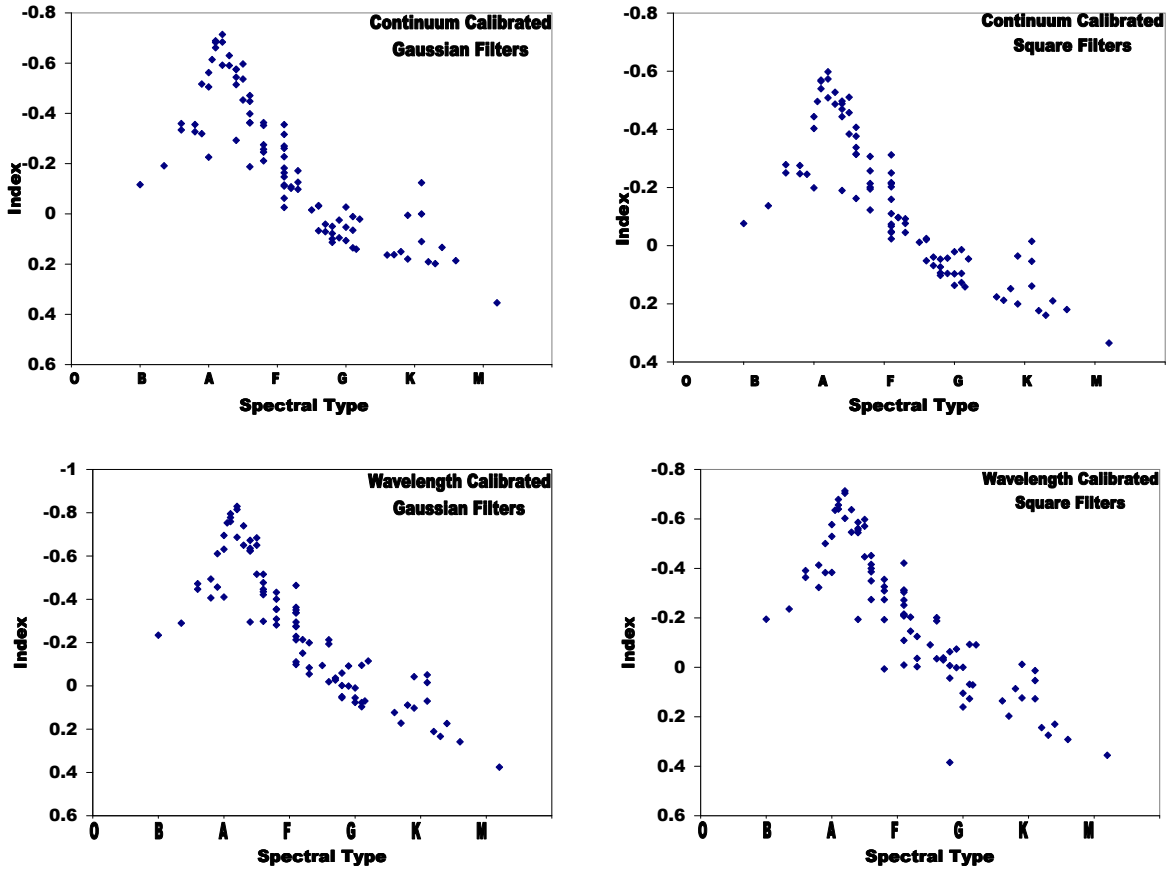

Figure 3.3: Ca II K-H index vs spectral type. The top left is continuum calibrated spectra and Gaussian filters, the top right is continuum calibrated spectra and square filters, the bottom left is wavelength calibrated spectra and Gaussian filters, and the bottom right is wavelength calibrated spectra and square filters.

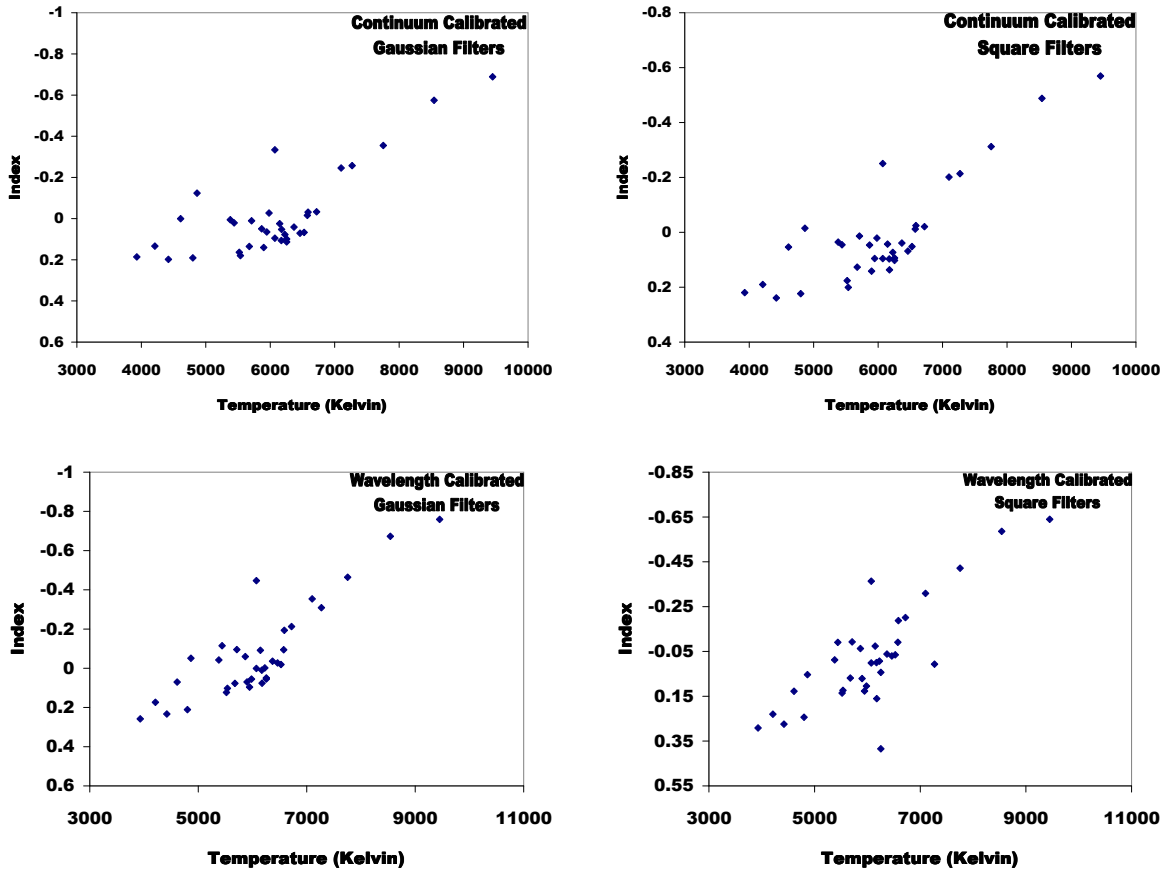

Figure 3.4: Ca II K-H index vs temperature. The top left is continuum calibrated spectra and Gaussian filters, the top right is continuum calibrated spectra and square filters, the bottom left is wavelength calibrated spectra and Gaussian filters, and the bottom right is wavelength calibrated spectra and square filters.

We inverted the x and y axes on both the temperature and spectral type plots for the wavelength calibrated spectra and Gaussian filters. We fitted a line to the temperature plot and two second order polynomials to the spectral type plot (separate polynomials for the stars above and below spectral type A0). Figure 3.5 shows those plots. The equation for the temperature plot was

$$y = -4056.69(\pm 425.33) \times x + 5784.862(\pm 103.10), \tag{3.1}$$

with an R^2 value of 0.7338. For the spectral type plot, the equation for the stars cooler than A0 was

$$y = 26.644(\pm 4.38) \times x^2 + 44.293(\pm 2.80) \times x + 40.880(\pm 0.52), \tag{3.2}$$

with an R2 value of 0.87. For the stars hotter than A0, the equation was

$$y = -46.689(\pm 19.11) \times x^2 - 62.904(\pm 19.34) \times x - 1.100(\pm 4.62), \tag{3.3}$$

with an R^2 value of 0.7878. There is the problem in the spectral type relation of which side of the curve to use, but if the Ca II K-H data were combined with a monotonic color index such as b-y, that should make the choice obvious.

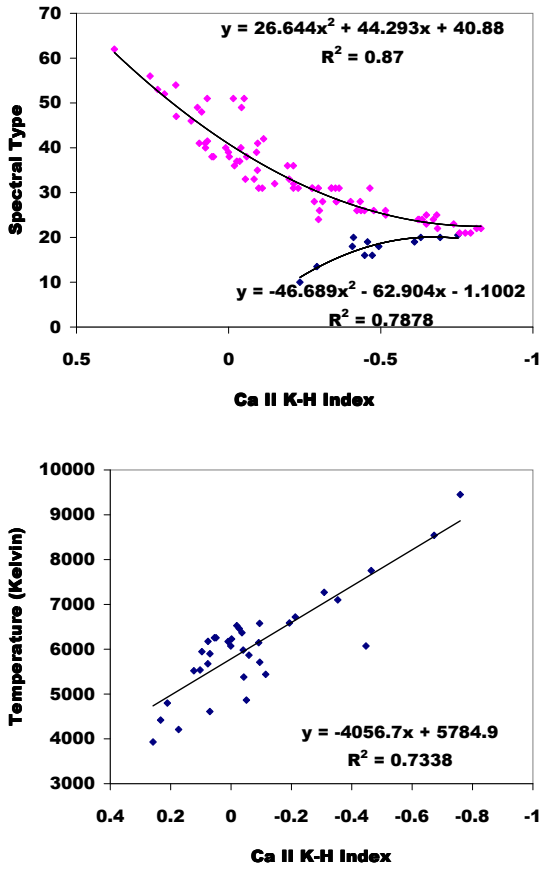

Figure 3.5: The plot on top is spectral type vs the Ca II K-H index. The plot on the bottom is temperature vs the Ca II K-H index. Points shown as green triangles were not included in the fits.

3.3 The Ca II HK-K Index

The Ca II HK-K index is defined as the magnitude through the wide filter covering both the Ca II H and K lines minus the magnitude through the narrow filter covering just the Ca II K line. This index also has a high correlation with temperature, but does not have as wide a magnitude range as the Ca II K-H index. Although reddening effects were not looked at in this study, it is likely that reddening has a slightly lower effect on this index than it does on the K-H index, as the two filters involved have central wavelengths that are even closer together.

Figure 3.6 shows the Ca II HK-K index vs spectral type. As in the Ca II K-H index, there is not much difference between the Gaussian and square filters, but there is a greater range in index values in the wavelength calibrated spectra than in the continuum calibrated spectra. There are, however, more outliers in the wavelength calibrated spectra.

Figure 3.7 shows the Ca II HK-K index vs temperature. This index does not appear to lose sensitivity quite as quickly as the K-H index for very hot and very cool stars. There is, once again, more scatter in the wavelength calibrated spectra than in the continuum calibrated spectra.

In the spectral type plots, the magnitude range for the continuum calibrated spectra and Gaussian filters is about 0.8, and the range for the continuum calibrated spectra and square filters is about 0.7. The range for the wavelength calibrated spectra and Gaussian filters is about 1.0 and the range for the wavelength calibrated spectra and square filters is about 0.8. In the temperature plots, the magnitude range for the continuum calibrated spectra and Gaussian filters is about 0.8, and the range for the continuum calibrated spectra and square filters is about 0.6. The range for the wavelength calibrated spectra and Gaussian filters is about 1.0, and the range for the wavelength calibrated spectra and square filters is about 0.9. As in the case of the Ca II K-H index, the wavelength calibrated spectra and Gaussian filters give the

widest magnitude range; however, the Ca II K-H index has a wider magnitude range with less scatter than this index.

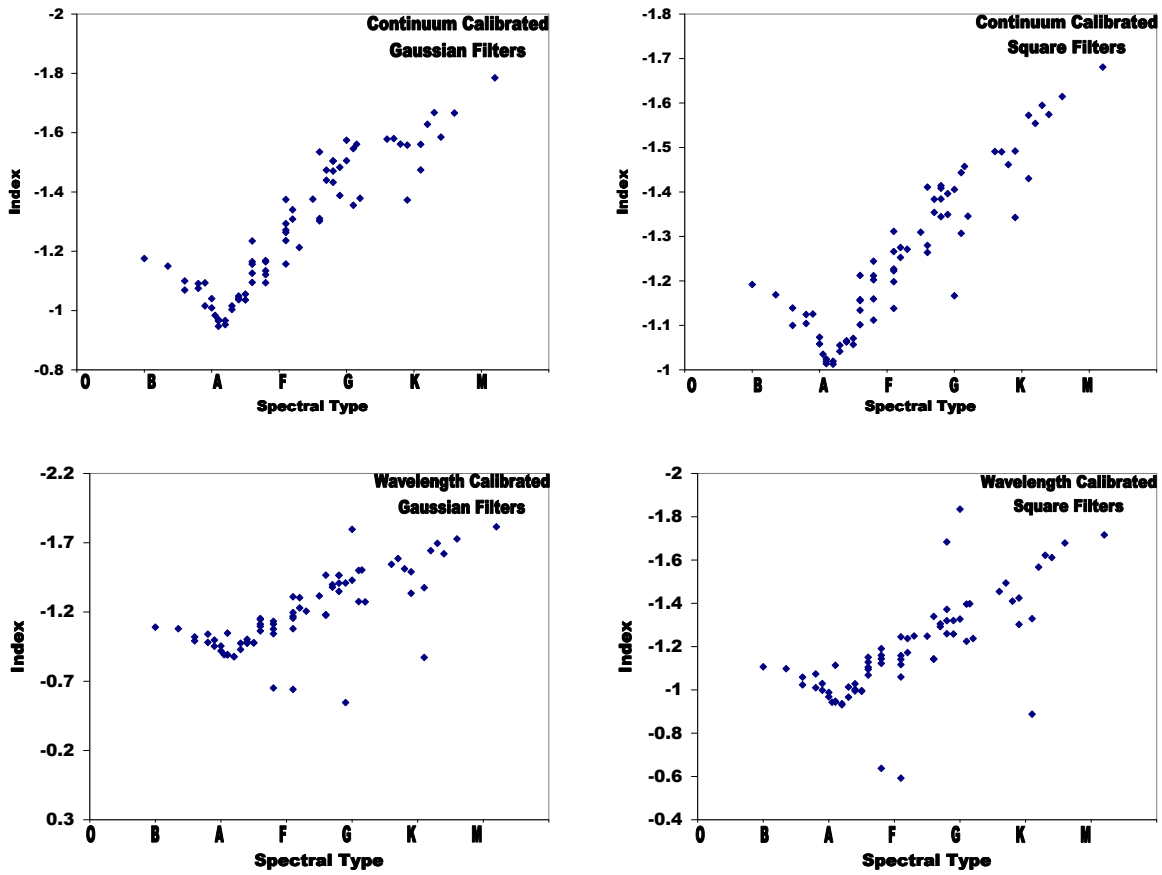

Figure 3.6: Ca II HK-K index vs spectral type. The top left is continuum calibrated spectra and Gaussian filters, the top right is continuum calibrated spectra and square filters, the bottom left is wavelength calibrated spectra and Gaussian filters, and the bottom right is wavelength calibrated spectra and square filters.

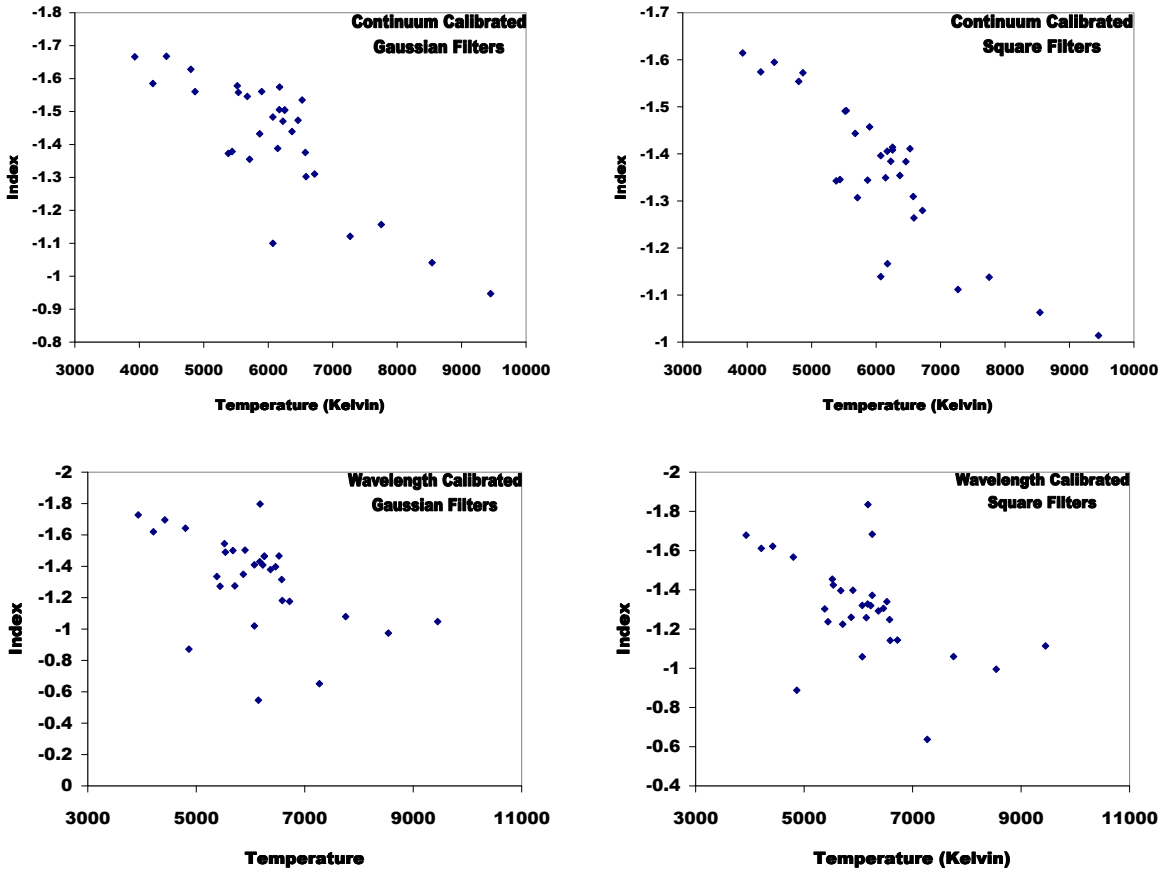

Figure 3.7: Ca II HK-K index vs temperature. The top left is continuum calibrated spectra and Gaussian filters, the top right is continuum calibrated spectra and square filters, the bottom left is wavelength calibrated spectra and Gaussian filters, and the bottom right is wavelength calibrated spectra and square filters.

Again, we inverted the axes and fitted a line to the temperature plot and second order polynomials to the spectral type plot. Figure 3.8 shows those plots. The equation for the temperature plot was

$$y = -1984.79(\pm 615.84) \times x + 8720.34(\pm 834.49), \tag{3.4}$$

with an R^2 value of 0.2637. For the spectral type plot, the equation for the stars cooler than A0 was

$$y = 35.06(\pm 7.66) \times x^2 + 58.80(\pm 18.90) \times x + 51.68(\pm 11.34), \tag{3.5}$$

with an R^2 value of 0.6635. For the stars hotter than A0, the equation was

$$y = -228.05(\pm 118.10) \times x^2 - 409.09(\pm 235.03) \times x - 163.30(\pm 116.63), \tag{3.6}$$

with an R^2 value of 0.8324.

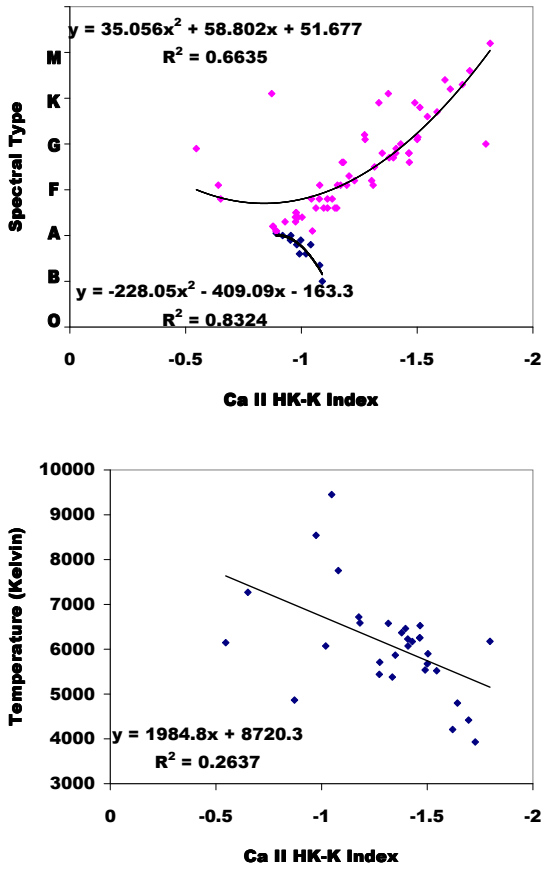

Figure 3.8: The plot on top is spectral type vs the Ca II HK-K index. The plot on the bottom is temperature vs the Ca II HK-K index. Points shown as green triangles were not included in the fits.

3.4 The Ca II HK-H Index

The Ca II HK-H index is defined as the magnitude through the wide filter covering both Ca II lines minus the magnitude of the narrow filter covering just the Ca II H line. This index appears to be much less useful than either the Ca II HK-K index or the Ca II K-H index, possibly as a result of the Ca II H line being blended with the Hϵ line.

Figure 3.9 shows the Ca II HK-H index vs spectral type. This index appears to lose sensitivity after about G0, but then the index values start increasing again for early to mid K stars. The fact the two preceding indices were two-valued will be dealt with in a later section, but it appears as though this index may actually be three-valued, although we don't really have enough data points to know for sure. There are quite a few outliers in the wavelength calibrated spectra.

Figure 3.10 shows the Ca II HK-H index vs temperature. There does not appear to be the correlation that would be needed to use this index as a temperature indicator.

In the spectral type plots, the continuum calibrated spectra and Gaussian filters have a magnitude range of about 0.4, and the continuum calibrated spectra and square filters have a magnitude range of about 0.35. The wavelength calibrated spectra and Gaussian filters have a range of about 0.5 and the wavelength calibrated spectra and square filters have a range of about 0.4. In the temperature plots, the continuum calibrated spectra and Gaussian filters have a range of about 0.3, and the continuum calibrated spectra and square filters also have a range of about 0.3. The wavelength calibrated spectra and Gaussian filters have a range of about 0.4, and the wavelength calibrated spectra and square filters also have a range of about 0.4. Again, the wavelength calibrated spectra and Gaussian filters have the widest magnitude ranges, but the ranges are much lower in this case than they were in the two previous indices.

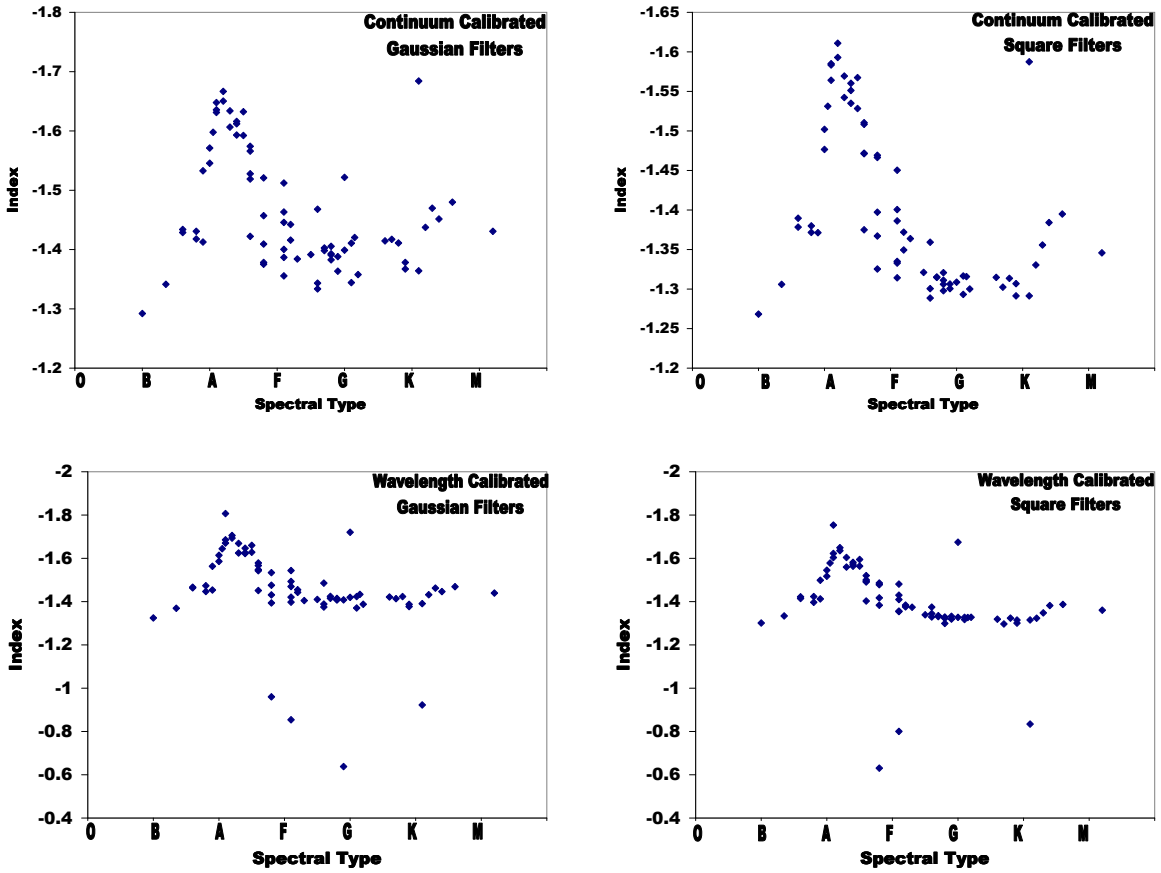

Figure 3.9: Ca II HK-H index vs spectral type. The top left is continuum calibrated spectra and Gaussian filters, the top right is continuum calibrated spectra and square filters, the bottom left is wavelength calibrated spectra and Gaussian filters, and the bottom right is wavelength calibrated spectra and square filters.

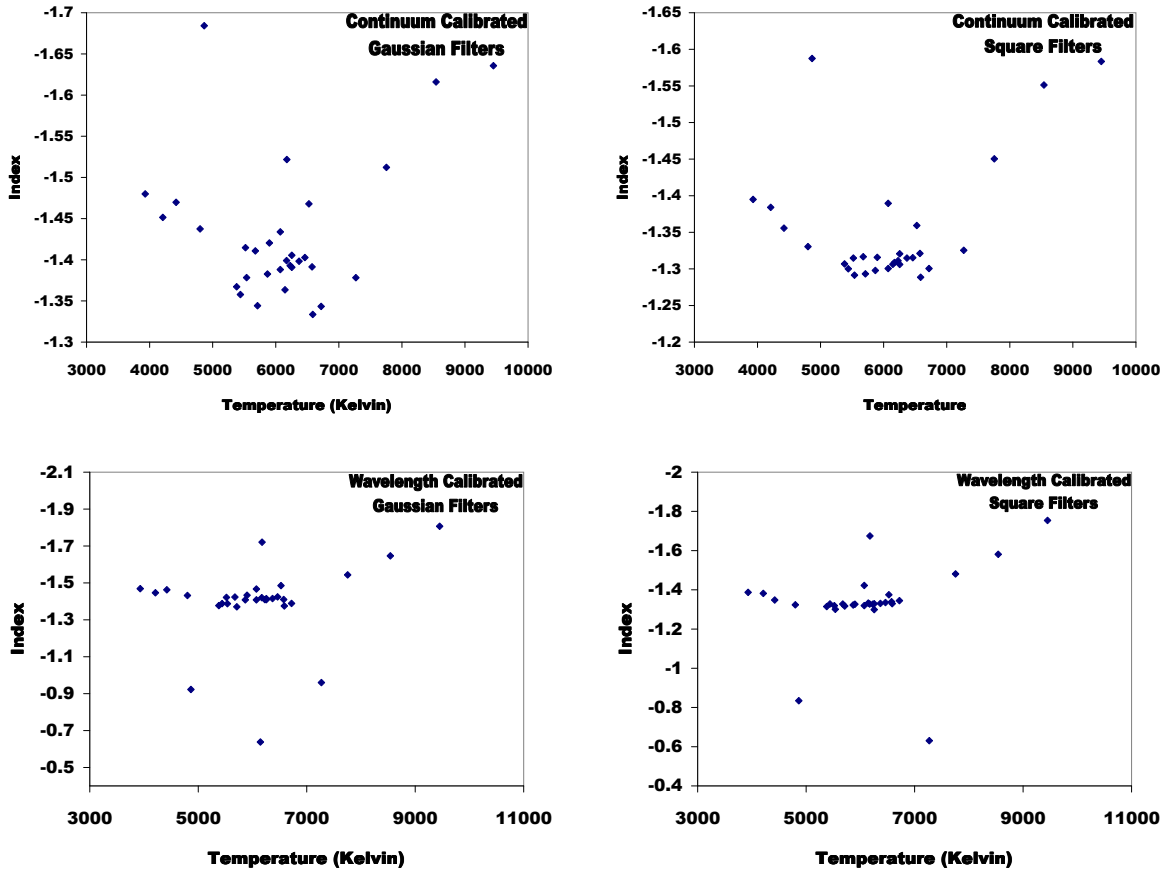

Figure 3.10: Ca II HK-H index vs temperature. The top left is continuum calibrated spectra and Gaussian filters, the top right is continuum calibrated spectra and square filters, the bottom left is wavelength calibrated spectra and Gaussian filters, and the bottom right is wavelength calibrated spectra and square filters.

Again, we inverted the axes and fitted a line to the temperature plot and second order polynomials to the spectral type plot. Figure 3.11 shows those plots. The equation for the temperature plot was

$$y = -8572.05(\pm 1904.76) \times x - 6305(\pm 2759.69), \tag{3.7}$$

with an R^2 value of 0.4476. For the spectral type plot, the equation for the stars cooler than A0 was

$$y = 60.00(\pm 94.49) \times x^2 + 251.26(\pm 292.21) \times x + 275.28(\pm 224.75), \tag{3.8}$$

with an R^2 value of 0.4745. For the stars hotter than A0, the equation was

$$y = -109.63(\pm 37.20) \times x^2 - 355.29(\pm 111.01) \times x - 267.76(\pm 82.57), \tag{3.9}$$

with an R^2 value of 0.8957.

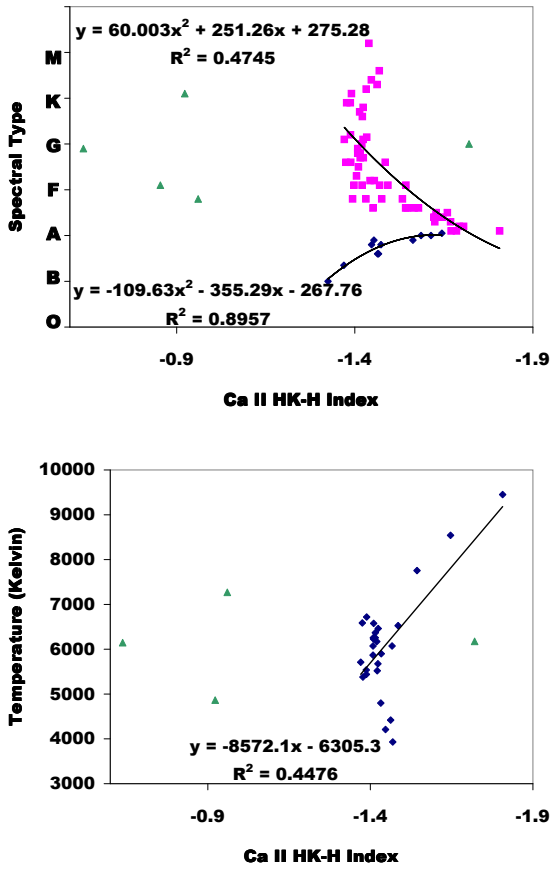

Figure 3.11: The plot on top is spectral type vs the Ca II HK-H index. The plot on the bottom is temperature vs the Ca II HK-H index. Points shown as green triangles were not included in the fits.

3.5 The Hδ Index

We define the Hδ index as the magnitude through the narrow filter centered on the Hδ line minus the magnitude through the wide filter centered on the Hδ, similar to the Hβ index. Figure 3.12 shows the Hδ index vs spectral type, and Figure 3.13 shows the Hδ index vs temperature.

As we saw for the Hβ index, there appears to be a strong correlation between the index values and the spectral type and temperature. In the spectral type plots, the index values for the continuum calibrated spectra and Gaussian filters have a magnitude range of about 0.5, and the values for the continuum calibrated spectra and square filters have a range of about 0.6. The values for the wavelength calibrated spectra and Gaussian filters have a range of about 0.6, and the values for the wavelength calibrated spectra and square filters have a range of about 0.5. In the temperature plots, the values for the continuum calibrated spectra and Gaussian filters have a range of about 0.5, and the values for the continuum calibrated spectra and square filters have a range of about 0.6. The values for the wavelength calibrated spectra and Gaussian filters have a range of about 0.6, and the values for the wavelength calibrated spectra and square filters have a range of about 0.5. Again, the wavelength calibrated spectra and Gaussian filters have the widest magnitude range, although it is not as high as the range was for either the Ca II K-H index or the Ca II HK-K index. It is comparable to the range of the Ca II HK-H index, but there appears to be a much stronger relation between the Hδ index and spectral type/temperature than there was for the Ca II HK-H index. This index also appears to lose sensitivity for cooler stars a bit sooner than the Ca II indices did. It loses sensitivity for hot stars at about the same place that the Ca II indices did, which we would expect because for hot stars the Ca II indices are basically Hϵ indices.

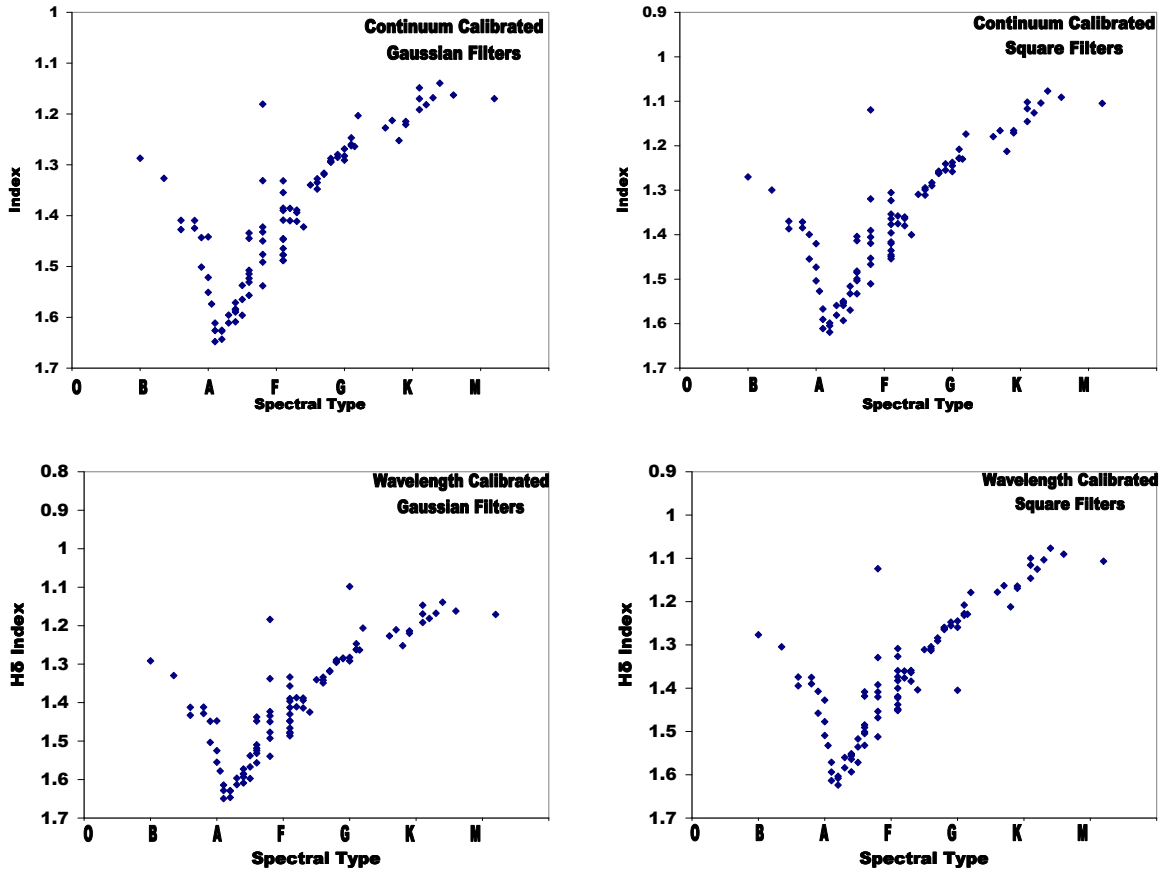

Figure 3.12: Hδ index vs spectral type. The top left is continuum calibrated spectra and Gaussian filters, the top right is continuum calibrated spectra and square filters, the bottom left is wavelength calibrated spectra and Gaussian filters, and the bottom right is wavelength calibrated spectra and square filters.

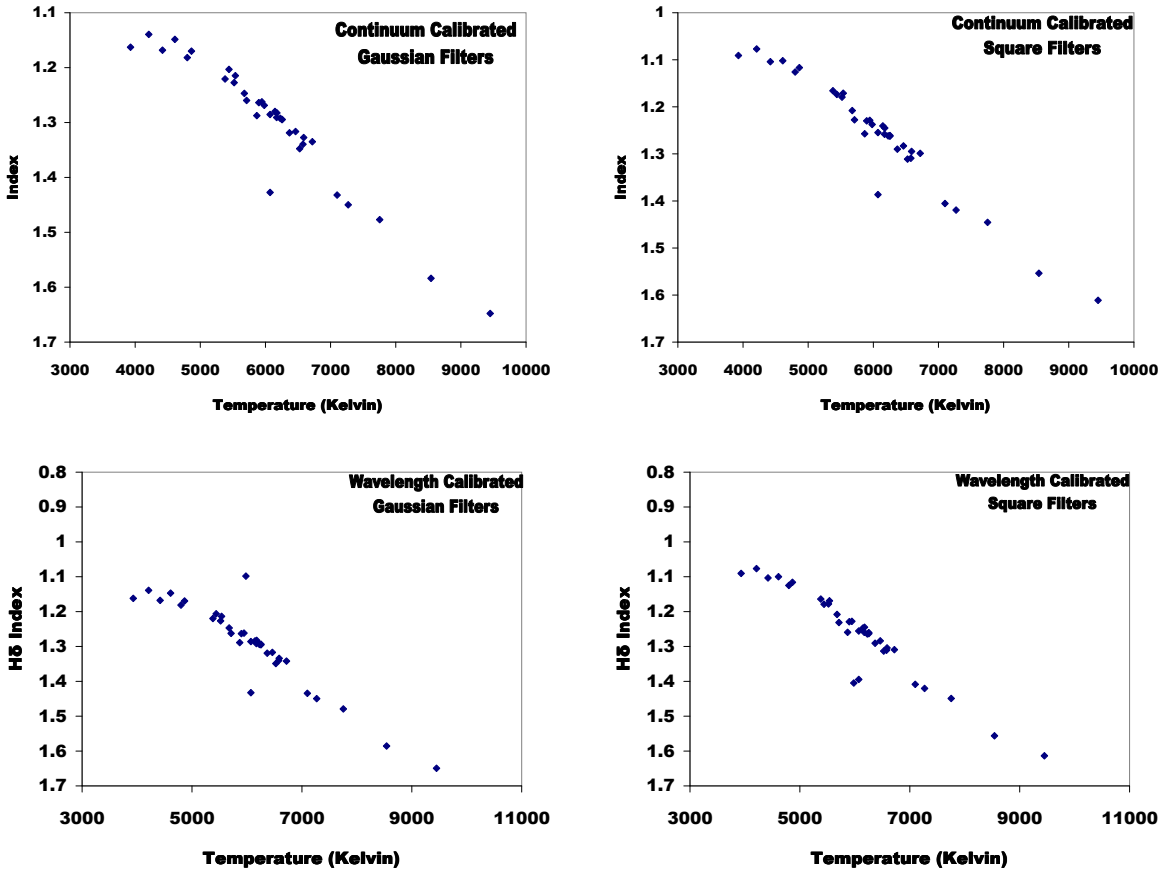

Figure 3.13: Hδ index vs temperature. The top left is continuum calibrated spectra and Gaussian filters, the top right is continuum calibrated spectra and square filters, the bottom left is wavelength calibrated spectra and Gaussian filters, and the bottom right is wavelength calibrated spectra and square filters.

Again, we inverted the axes and fitted a line to the temperature plot and second order polynomials to the spectral type plot. Figure 3.14 shows those plots. The equation for the temperature plot was

$$y = -9603.69(\pm 374.61) \times x - 6375.67(\pm 487.56), \tag{3.10}$$

with an R^2 value of 0.9550. For the spectral type plot, the equation for the stars cooler than A0 was

$$y = 113.57(\pm 14.08) \times x^2 - 380.26(\pm 39.46) \times x + 341.28(\pm 27.43), \tag{3.11}$$

with an R^2 value of 0.9351. For the stars hotter than A0, the equation was

$$y = -131.40(\pm 39.10) \times x^2 - 411.33(\pm 112.54) \times x - 301.71(\pm 80.83), \tag{3.12}$$

with an R^2 value of 0.9106.

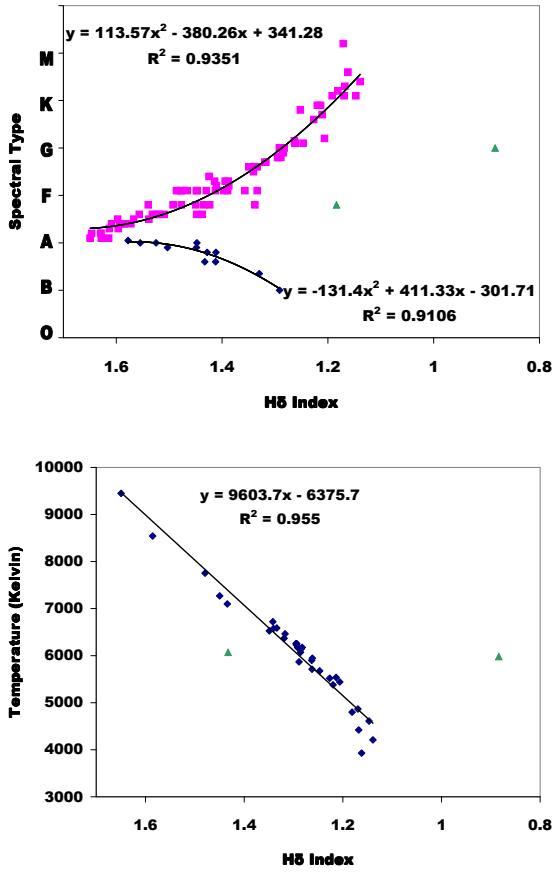

Figure 3.14: The plot on top is spectral type vs the Hδ index. The plot on the bottom is temperature vs the Hδ index. Points shown as green triangles were not included in the fits.

3.6 The Hγ Index

We define the Hγ index as the magnitude through the narrow filter centered on the Hγ line minus the magnitude through the wide filter centered on the Hγ, similar to the Hβ index. Figure 3.15 shows the Hγ index vs spectral type, and Figure 3.16 shows the Hγ index vs temperature.

As in the case of the other two hydrogen indices, Hβ and Hγ, there appears to be a strong correlation between the Hγ index and spectral type/temperature. In the spectral type plots, the continuum calibrated spectra and Gaussian filters have a magnitude range of about 0.6, and the continuum calibrated spectra and square filters have a magnitude range of about 0.5. The wavelength calibrated spectra and Gaussian filters have a magnitude range of about 0.6, and the wavelength calibrated spectra and square filters also have a range of about 0.6. In the temperature plots, the continuum calibrated spectra and Gaussian filters have a range of about 0.5, and the continuum calibrated spectra and square filters have a range of about 0.45. The wavelength calibrated spectra and Gaussian filters have a range of about 0.5, and the wavelength calibrated spectra and square filters also have a range of about 0.5. As in the case of the Hδ index, the Hγ index appears to lose sensitivity sooner than the Ca II indices did. The wavelength calibrated spectra have a slightly higher range than the continuum calibrated spectra, but there was not much difference between the Gaussian and square filters. The range is about the same as it was for the Hδ index. There appears to be a bit more scatter in the Hγ plots than there was in the Hδ plots.

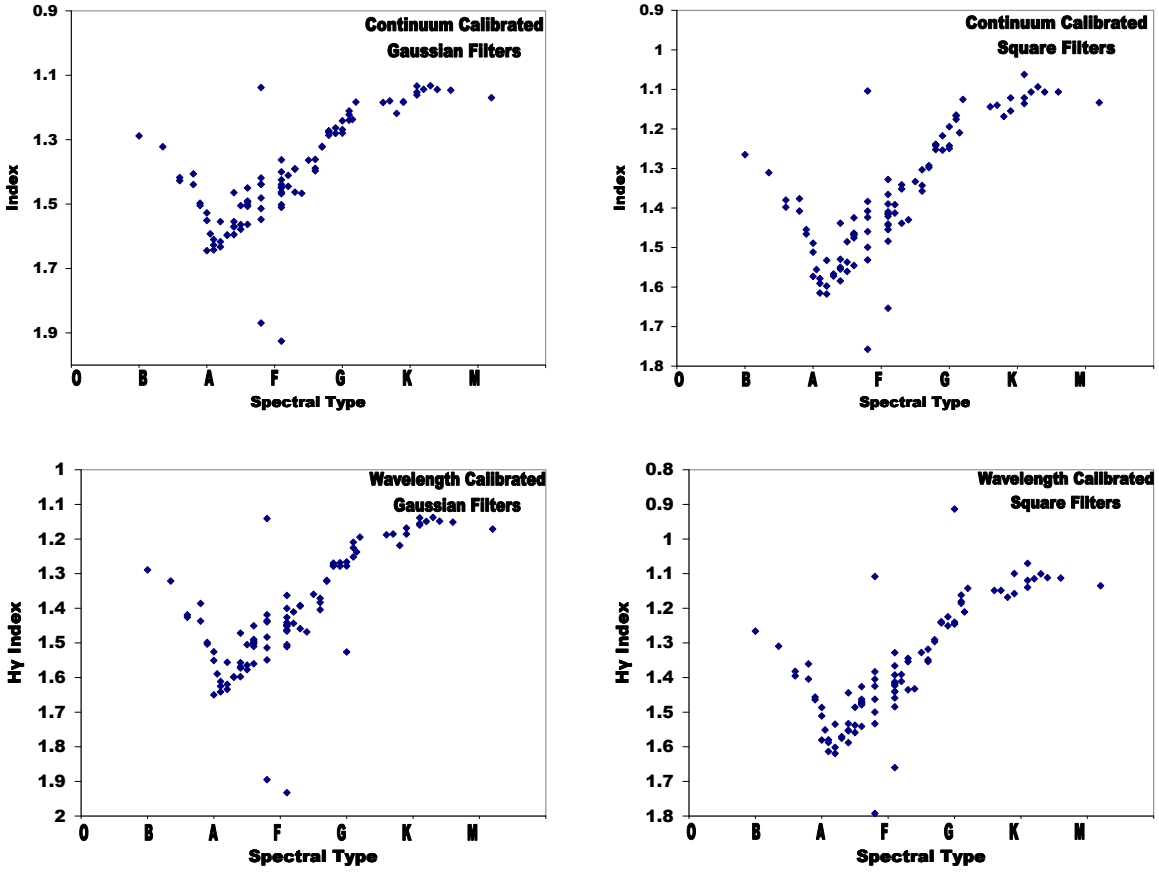

Figure 3.15: Hγ index vs spectral type. The top left is continuum calibrated spectra and Gaussian filters, the top right is continuum calibrated spectra and square filters, the bottom left is wavelength calibrated spectra and Gaussian filters, and the bottom right is wavelength calibrated spectra and square filters.

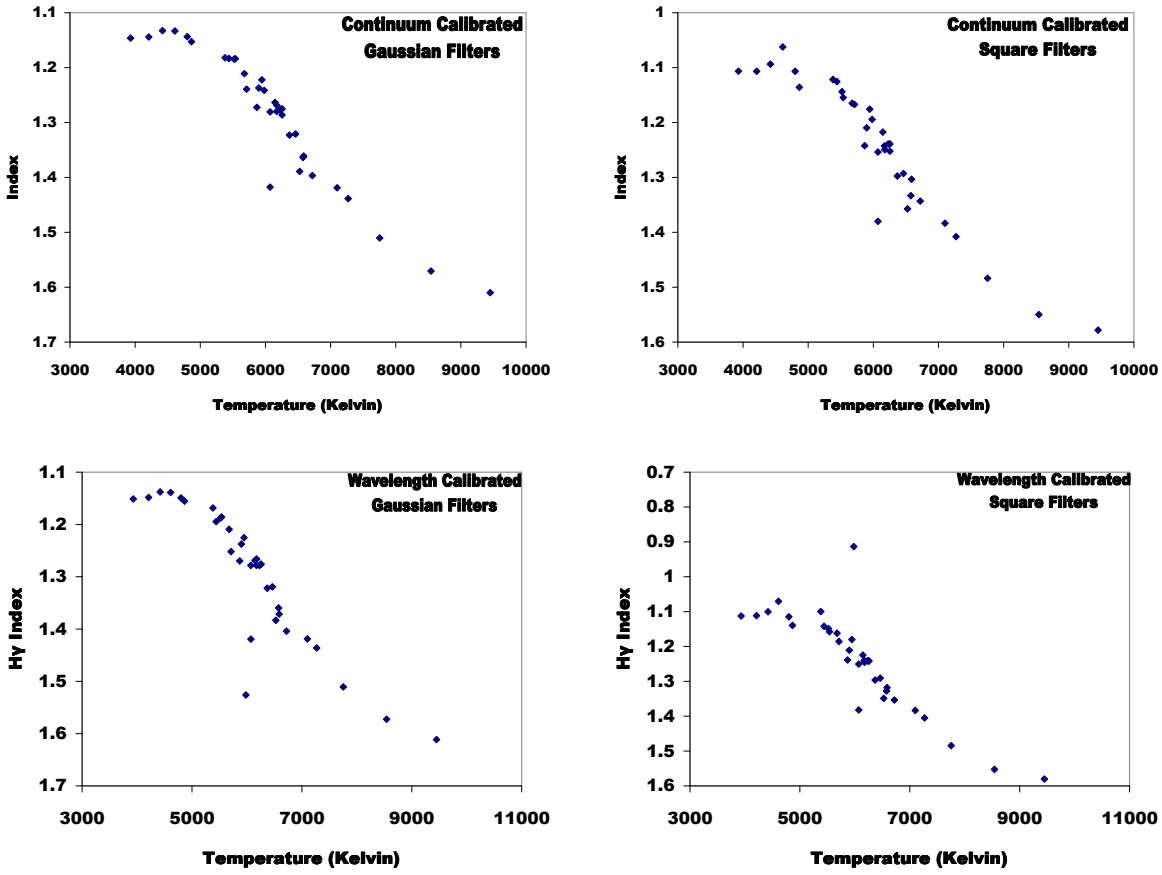

Figure 3.16: Hγ index vs temperature. The top left is continuum calibrated spectra and Gaussian filters, the top right is continuum calibrated spectra and square filters, the bottom left is wavelength calibrated spectra and Gaussian filters, and the bottom right is wavelength calibrated spectra and square filters.

Again, we inverted the axes and fitted a line to the temperature plot and second order polynomials to the spectral type plot. Figure 3.17 shows those plots. The equation for the temperature plot was

$$y = 8905.90(\pm 467.54) \times x - 5379.11(\pm 603.99), \tag{3.13}$$

with an R^2 value of 0.9213. For the spectral type plot, the equation for the stars cooler than A0 was

$$y = 66.997(\pm 13.15) \times x^2 - 244.50(\pm 36.32) \times x + 243.11(\pm 24.84), \tag{3.14}$$

with an R^2 value of 0.9413. For the stars hotter than A0, the equation was

$$y = -95.12(\pm 25.61) \times x^2 + 304.78(\pm 75.09) \times x - 223.89(\pm 54.85), \tag{3.15}$$

with an R^2 value of 0.9138.

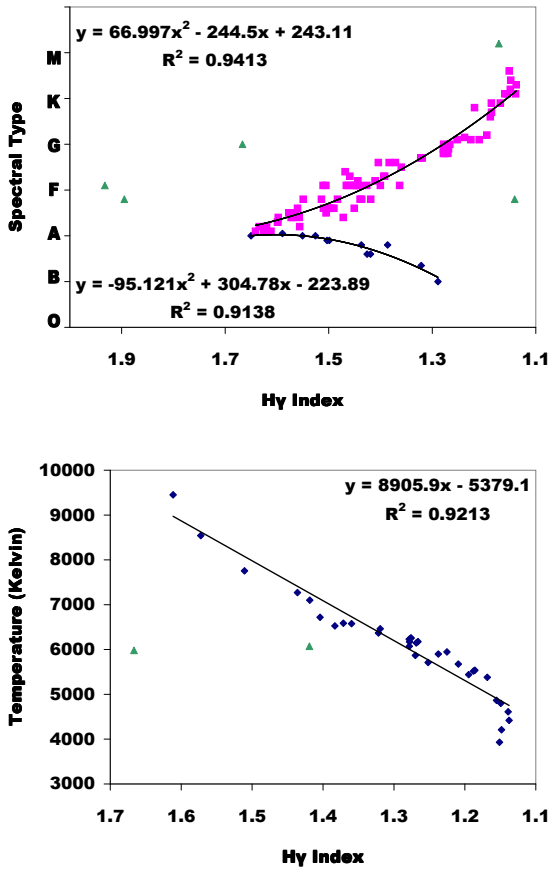

Figure 3.17: The plot on top is spectral type vs the Hγ index. The plot on the bottom is temperature vs the Hγ index. Points shown as green triangles were not included in the fits.

3.7 The Ca II (K-H) - Hδ Index

The Ca II (K-H) - Hδ index is defined as the Ca II K-H index value minus the Hδ index value. In this case, since the Ca II lines and the Hδ line are fairly far apart in wavelength, we would not expect this index to be reddening free. Figure 3.18 shows the Ca II (K-H) - Hδ index vs spectral type. Figure 3.19 shows the Ca II (K-H) - Hδ index vs temperature.

In the spectral type plots, the magnitude range for the continuum calibrated spectra and Gaussian filters is about 1.5 magnitudes, and the range for continuum calibrated spectra and square filters is about 1.4 magnitudes. The magnitude range for wavelength calibrated spectra and Gaussian filters is about 1.6 magnitudes, and the range for wavelength calibrated spectra and square filters is about 1.5 magnitudes.

In the temperature plots, the magnitude range for the continuum calibrated spectra and Gaussian filters is about 1.4, and the range for continuum calibrated spectra and square filters is about 1.5. The range for wavelength calibrated spectra and Gaussian filters is about 1.6, and the range for wavelength calibrated spectra and square filters is about 1.5. In both the spectral type plots and the temperature plots, the wavelength calibrated spectra and Gaussian filters have the widest magnitude range.

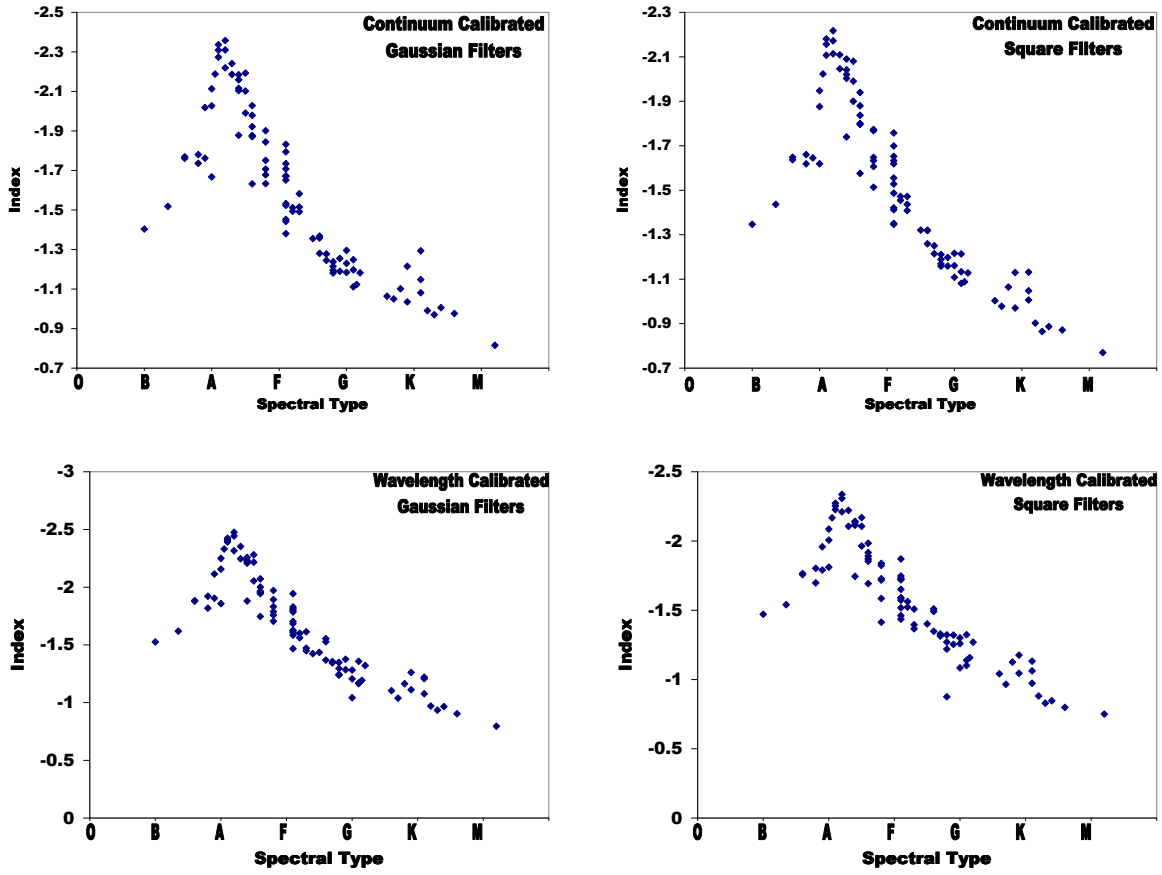

Figure 3.18: Ca II (K-H) - Hδ index vs spectral type. The top left is continuum calibrated spectra and Gaussian filters, the top right is continuum calibrated spectra and square filters, the bottom left is wavelength calibrated spectra and Gaussian filters, and the bottom right is wavelength calibrated spectra and square filters.

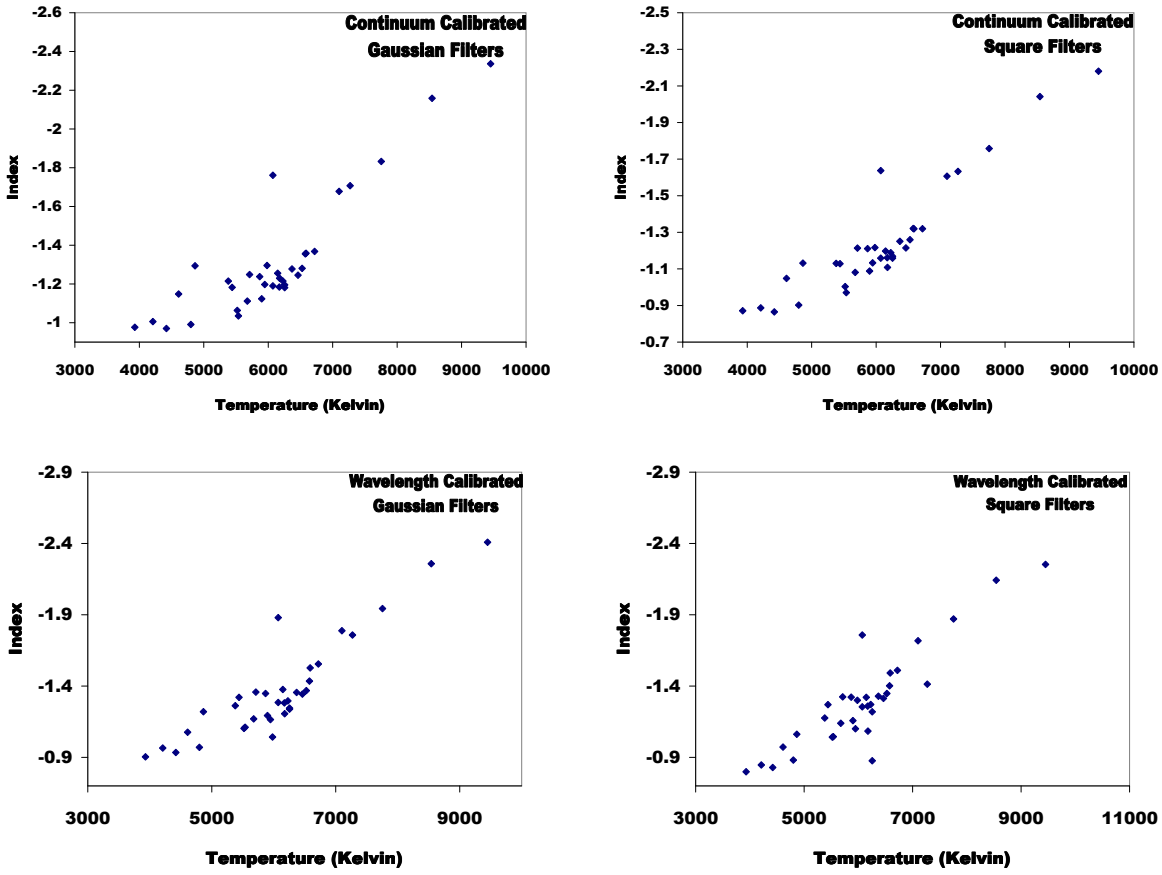

Figure 3.19: Ca II (K-H) - Hδ index vs temperature. The top left is continuum calibrated spectra and Gaussian filters, the top right is continuum calibrated spectra and square filters, the bottom left is wavelength calibrated spectra and Gaussian filters, and the bottom right is wavelength calibrated spectra and square filters.

Again, we inverted the axes and fitted a line to the temperature plot and second order polynomials to the spectral type plot. Figure 3.20 shows those plots. The equation for the temperature plot was

$$y = -3139.81(\pm 208.10) \times x - 1814.87(\pm 290.96), \tag{3.16}$$

with an R^2 value of 0.8801. For the spectral type plot, the equation for the stars cooler than A0 was

$$y = 12.26(\pm 1.75) \times x^2 + 61.18(\pm 5.92) \times x + 98.91(\pm 4.75), \tag{3.17}$$

with an R^2 value of 0.9056. For the stars hotter than A0, the equation was

$$y = -18.88(\pm 6.60) \times x^2 - 84.32(\pm 25.65) \times x - 74.01(\pm 24.69), \tag{3.18}$$

with an R^2 value of 0.8466.

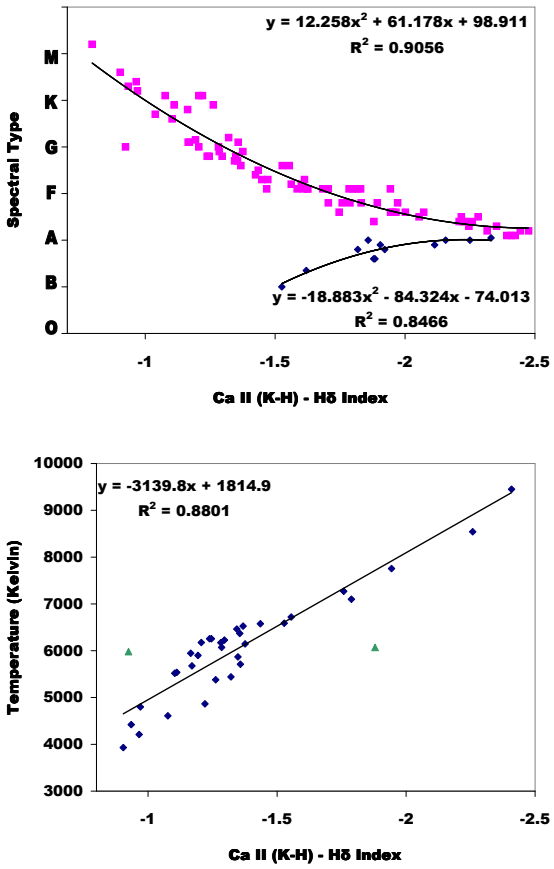

Figure 3.20: The plot on top is spectral type vs the Ca II (K-H) - Hδ index. The plot on the bottom is temperature vs the Ca II (K-H) - Hδ index. Points shown as green triangles were not included in the fits.

3.8 The Ca II (K-H) - Hγ Index

The Ca II (K-H) - Hγ index is defined as the Ca II K-H index value minus the Hγ index value. Again, as with the Ca II (K-H) - Hδ index, we would not expect this index to be reddening free. Figure 3.21 shows the Ca II (K-H) - Hγ index vs spectral type. Figure 3.22 shows the Ca II (K-H) - Hγ index vs temperature.

In the spectral type plots, the magnitude range for the continuum calibrated spectra and Gaussian filters is about 1.6, and the range for the continuum calibrated spectra and square filters is about 1.4. The magnitude range for the wavelength calibrated spectra and Gaussian filters is about 1.7, and the magnitude range for the wavelength calibrated spectra and square filters is about 2.0.

In the temperature plots, the magnitude range for the continuum calibrated spectra and Gaussian filters is about 1.4, and the magnitude range for the continuum calibrated spectra and square filters is about 1.3. The magnitude range for the wavelength calibrated spectra and Gaussian filters is about 1.7, and the magnitude range for the wavelength calibrated spectra and square filters is about 2.0. For this index, the wavelength calibrated spectra and square filters seem to have the widest magnitude range.

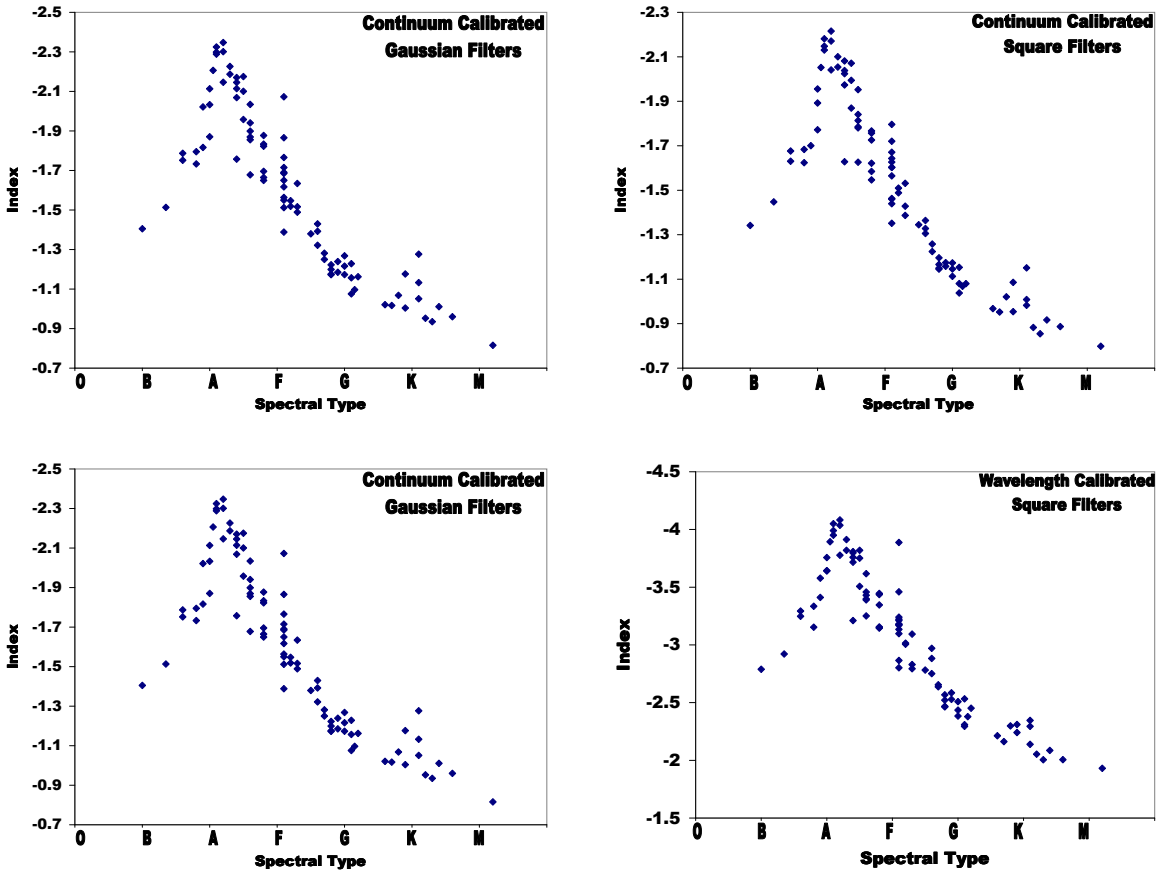

Figure 3.21: Ca II (K-H) - Hγ index vs spectral type. The top left is continuum calibrated spectra and Gaussian filters, the top right is continuum calibrated spectra and square filters, the bottom left is wavelength calibrated spectra and Gaussian filters, and the bottom right is wavelength calibrated spectra and square filters.

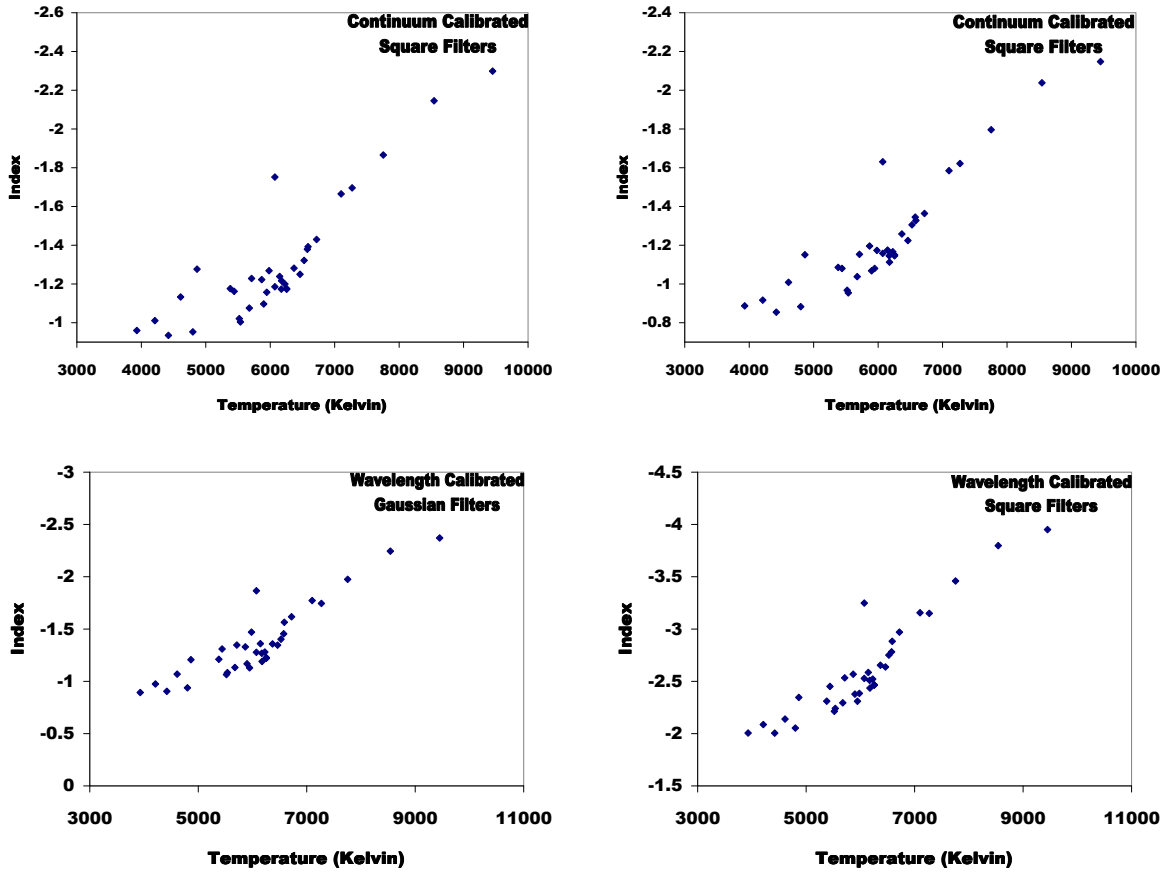

Figure 3.22: Ca II (K-H) - Hγ index vs temperature. The top left is continuum calibrated spectra and Gaussian filters, the top right is continuum calibrated spectra and square filters, the bottom left is wavelength calibrated spectra and Gaussian filters, and the bottom right is wavelength calibrated spectra and square filters.

Again, we inverted the axes and fitted a line to the temperature plot and second order polynomials to the spectral type plot. Figure 3.23 shows those plots. The equation for the temperature plot was

$$y = -3079.79(\pm 208.42) \times x + 1928.09(\pm 289.62), \tag{3.19}$$

with an R^2 value of 0.8757. For the spectral type plot, the equation for the stars cooler than A0 was

$$y = 12.51(\pm 1.76) \times x^2 + 61.81(\pm 5.91) \times x + 99.46(\pm 4.72), \tag{3.20}$$

with an R^2 value of 0.9068. For the stars hotter than A0, the equation was

$$y = -15.13(\pm 5.08) \times x^2 - 70.11(\pm 19.65) \times x - 60.92(\pm 18.82), \tag{3.21}$$

with an R^2 value of 0.9061.

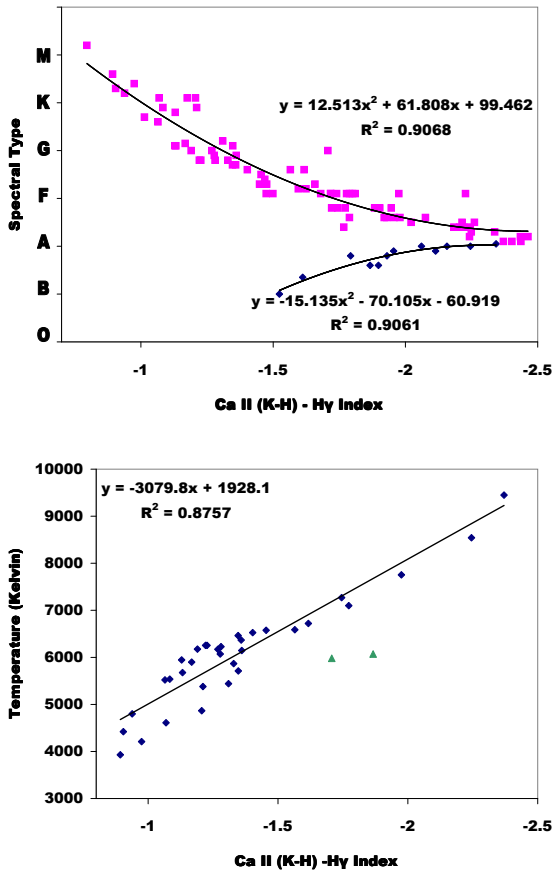

Figure 3.23: The plot on top is spectral type vs the Ca II (K-H) - Hγ index. The plot on the bottom is temperature vs the Ca II (K-H) - Hγ index. Points shown as green triangles were not included in the fits.

3.9 Arcturus

For some reason, the one star that really did not fit in any of our relations was Arcturus (α Boo). It is slightly variable and it is a giant star, but we have other variables in our data set and other giant stars, and all of those stars fit in our relations pretty well. In the plots with the wavelength calibrated spectra, Arcturus was below the rest of the data points, and in the plots with the continuum calibrated spectra, Arcturus was above the rest of the data points. Arcturus is a bright star and we have a large number of observations of it, and there is no obvious reason why it should not fit with the rest of the stars. Arcturus is the brightest star in our data set (magnitude -0.04), so it is likely that the spectra were simply overexposed. Because of this, however, in order to better examine the relations that worked for the other 94 stars in our data set, Arcturus was removed from our plots.

3.10 Index Values vs Metallicity

The plots in Figures 3.24 and 3.25 show the index values vs metallicity for the five indices involving the Ca II lines (since we would not expect an index based on only hydrogen lines to be sensitive to metal content). In each case, the values for the wavelength calibrated spectra and Gaussian filters are shown. We do not see any obvious relation between the index values and metallicity, but this does not show conclusively that the Ca II temperature indices are not influenced by metallicity.

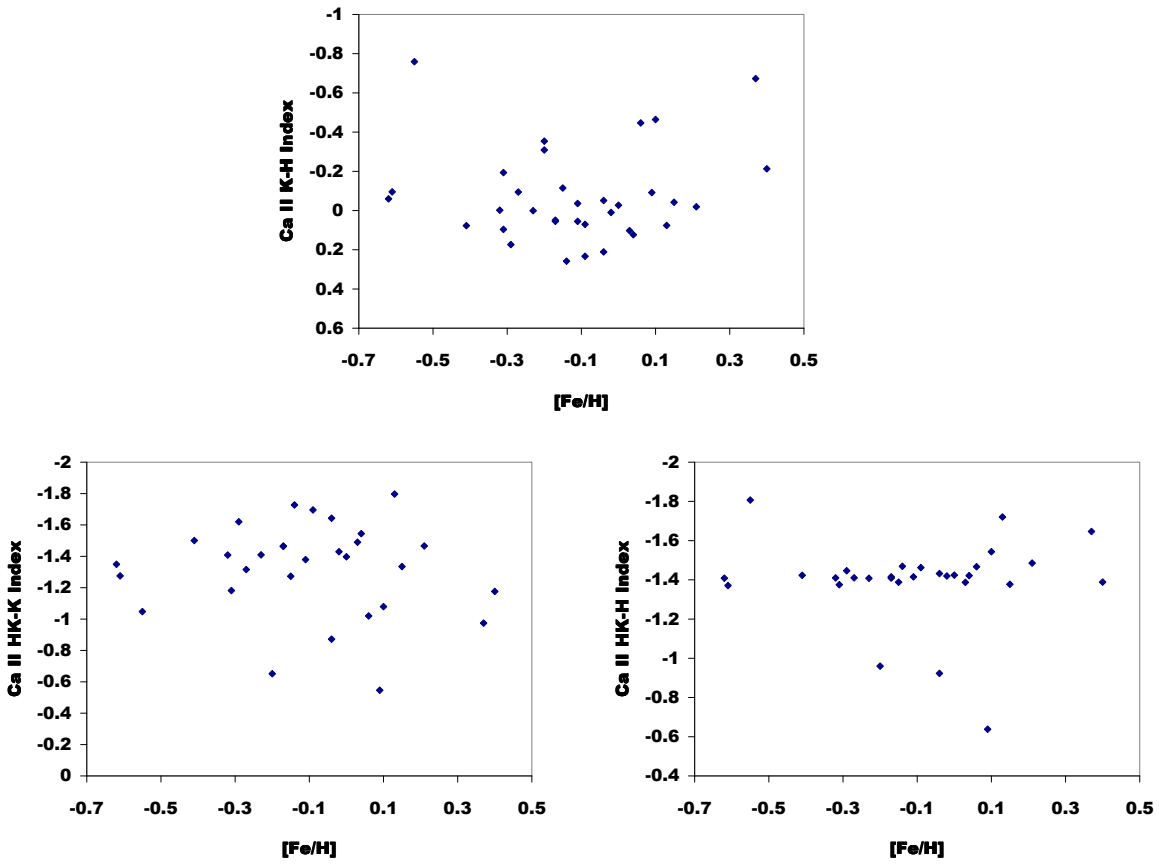

Figure 3.24: The plot at the top is the Ca II K-H index vs [Fe/H]. The plot at the bottom left is the Ca II HK-K index vs [Fe/H]. The plot at the bottom right is the Ca II HK-H index vs [Fe/H].

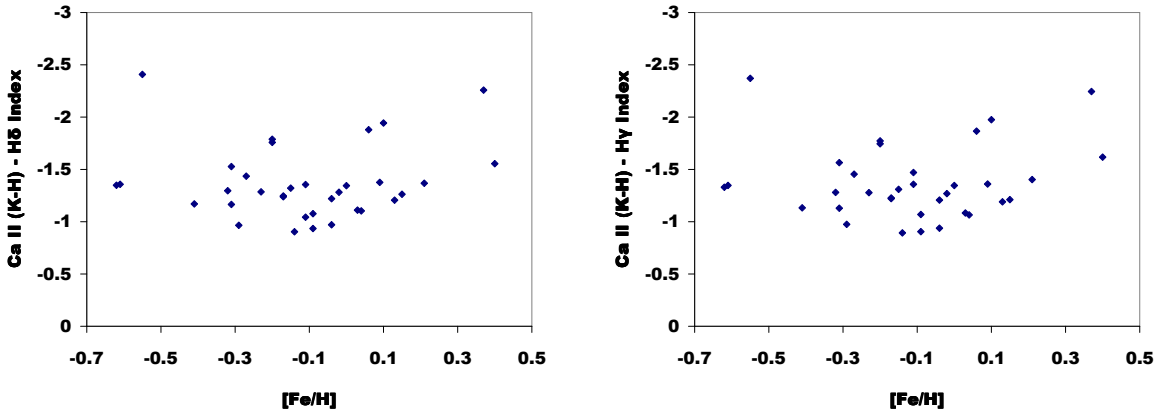

Figure 3.25: The plot on the left is the Ca II (K-H) - Hδ index vs [Fe/H]. The plot on the right is the Ca II (K-H) - Hγ index vs [Fe/H].

3.11 Comparing the Indices With Each Other

We plotted our seven indices versus the Hβ index and also compared some of them with each other. Table 3.2 shows the coefficient of determination, R^2, for all of the combinations that we compared. In all cases the index values shown are from wavelength calibrated spectra and Gaussian filters. Points shown as blue diamonds on the plots were included in the fits, and points shown as pink squares were not.

Table 3.2. Coefficients of determination for index comparisons

Indices	R^2
Hδ and Hβ	0.9655
Hγ and Hβ	0.9324
Hδ and Hγ	0.9478
Ca II K-H and Hβ	0.9093
Ca II HK-K and Hβ	0.5761
Ca II HK-H and Hβ	0.7112
Ca II (K-H) - Hδ and Hβ	0.8571
Ca II (K-H) - Hγ and Hβ	0.841
Ca II (K-H) - Hδ and Ca II (K-H) - Hγ	0.994
Hδ and Ca II (K-H) - Hδ	0.9287
Hγ and Ca II (K-H) - Hγ	0.9184
Ca II K-H and Ca II HK-K	0.9315
Ca II K-H and Ca II HK-H	0.648
Ca II HK-K and Ca II HK-H	0.2481
Ca II K-H and Hδ	0.8588
Ca II K-H and Hγ	0.9625

Figure 3.26 shows the Hδ index vs the Hβ index, the Hγ index vs the Hβ index, and the Hδ index vs the Hγ index. There is a higher correlation between Hδ and Hβ than there is between Hγ and Hβ.

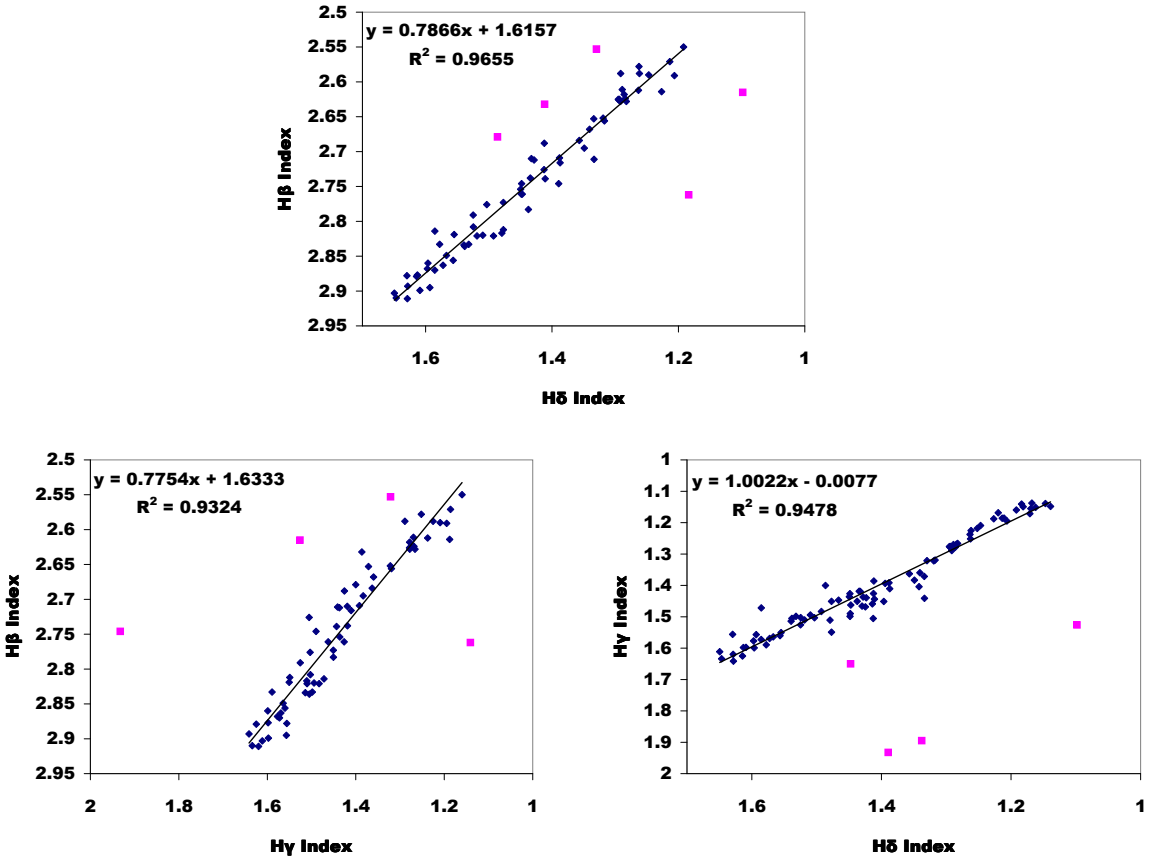

Figure 3.26: The plot on top shows the Hδ index vs the Hβ index. The plot on the bottom left shows the Hγ index vs the Hβ index. The plot on the bottom right shows the Hδ index vs the Hγ index.

Figure 3.27 shows the Ca II K-H, Ca II HK-K, and Ca II HK-H index vs the Hβ index. There is a fairly high correlation between the Ca II K-H index and the Hβ index, but not as high of a correlation between the Hβ index and the Ca II HK-K and Ca II HK-H indices. In the plot of the Ca II K-H index vs Hβ, there appears to be a second series of about 10 data points (shown as green diamonds), with an R^2 value of 0.9491. We are not sure what causes this line or whether it is even significant, but Figure 3.28 shows that is not related to either metallicity or spectral type.

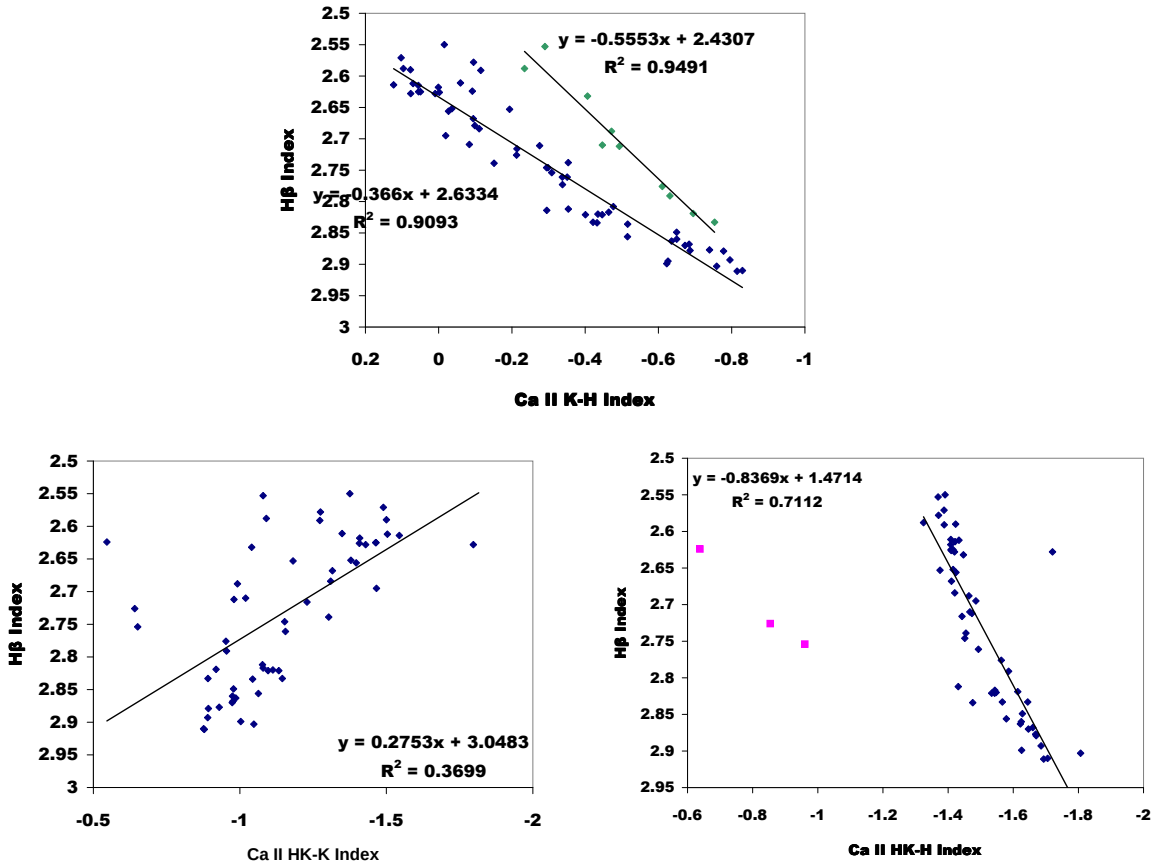

Figure 3.27: The plot on top shows the Ca II K-H index vs the Hβ index. The plot on the bottom left shows the Ca II HK-K index vs the Hβ index. The plot on the bottom right shows the Ca II HK-H index vs the Hβ index.

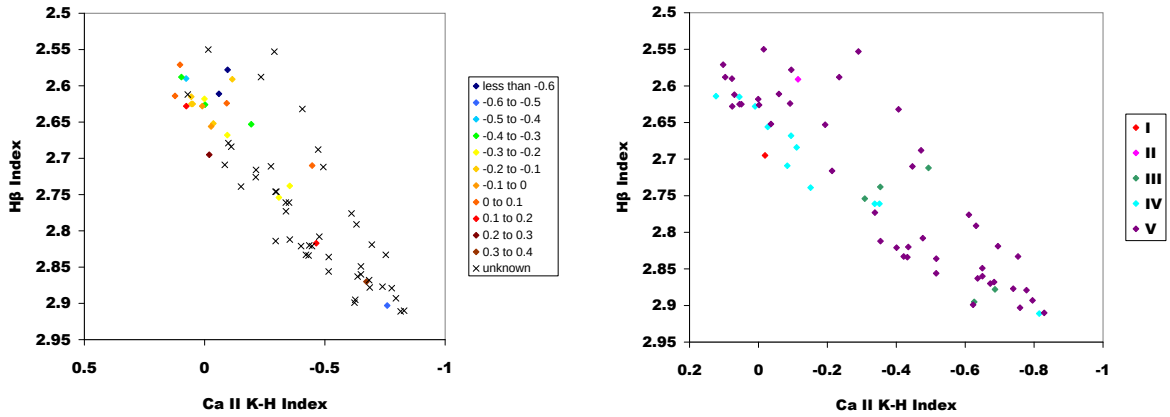

Figure 3.28: The plot on the left shows the Ca II K-H index vs the Hβ index with data points color coded according to [Fe/H]. The plot on the right shows the Ca II K-H index vs the Hβ index with data points color coded according to luminosity class. We see no trends involving [Fe/H] or luminosity class.

Figure 3.29 shows the Ca II (K-H) - Hδ and Ca II (K-H) - Hγ indices compared with each other, the Hβ index, and the Hδ and Hγ indices. The two indices have a high correlation with each other. They each have a fairly high correlation with the Hβ index, although it is higher for the Ca II (K-H) - Hδ index. The Ca II (K-H) - Hδ and Ca II (K-H) - Hγ indices have a very high correlation with each other. The Ca II (K-H) - Hδ and Hδ indices and the Ca II (K-H) - Hγ and Hγ indices also have high correlations with each other.

Figure 3.30 shows the Ca II K-H, HK-K, and HK-H indices compared with each other, as well as Ca II K-H compared with Hδ and Hγ. There is a higher correlation between the Ca II K-H index and Hδ than there is with Hγ. In the plot of Ca II HK-K vs HK-H, we can see that HK-H loses sensitivity much sooner than HK-K. There is a higher correlation between K-H and HK-K than between K-H and HK-H.

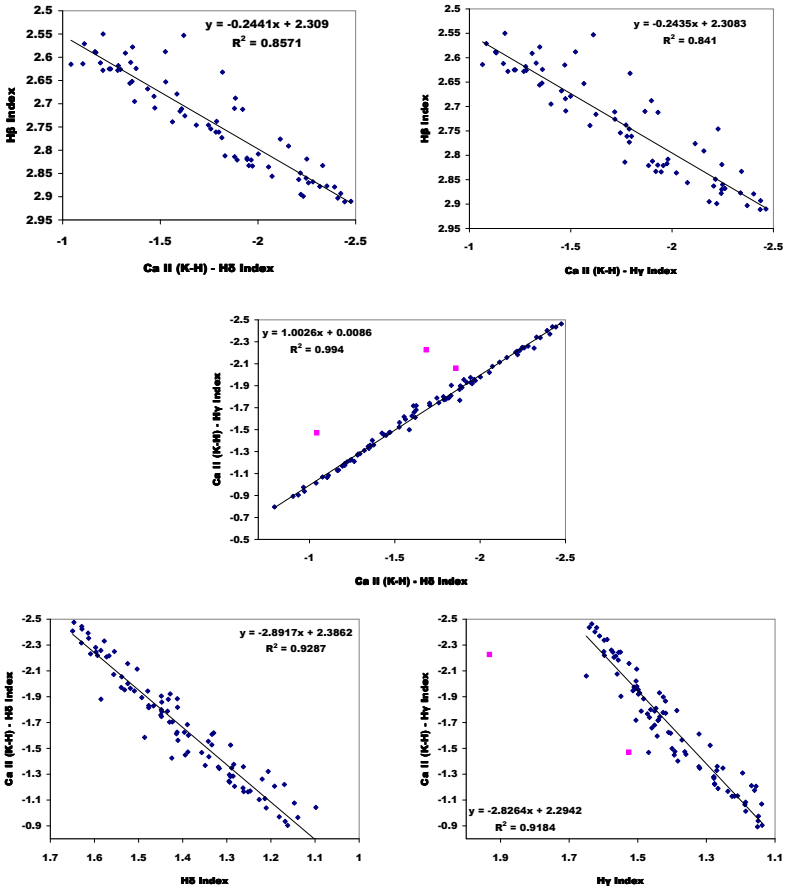

Figure 3.29: The plot on the top left is the Ca II (K-H) - Hδ index vs the Hβ index, the top right is the Ca II (K-H) - Hγ index vs the Hβ index, the center is the Ca II (K-H) - Hδ index vs the Ca II (K-H) - Hγ index, the bottom left is the Ca II (K-H) - Hδ index vs the Hδ index, and the bottom right is the Ca II (K-H) - Hγ index vs the Hγ index.

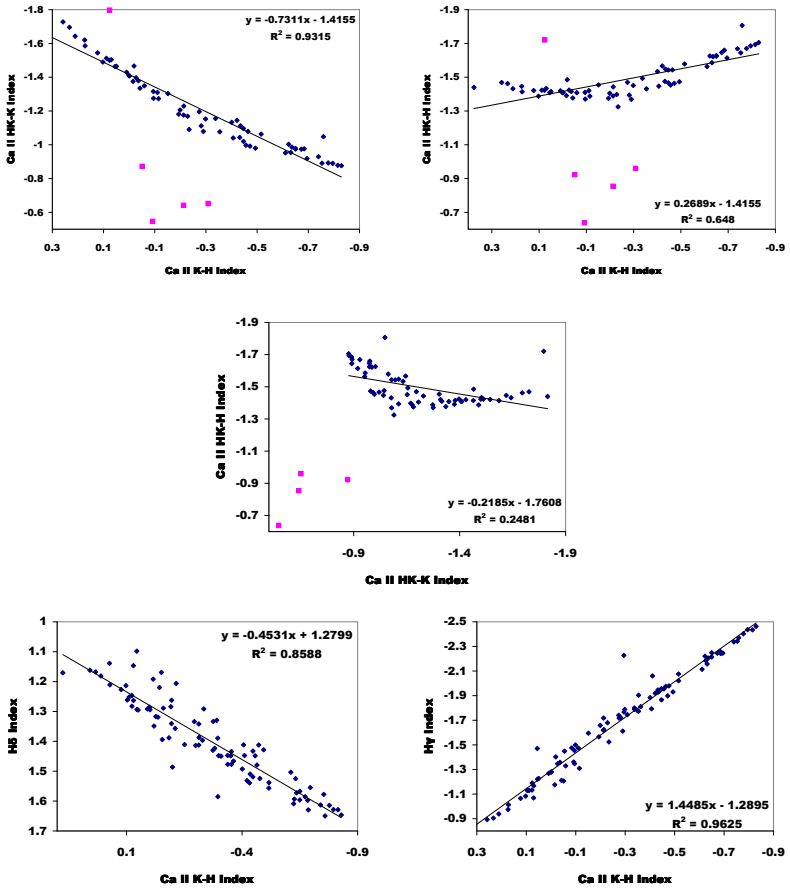

Figure 3.30: The plot on the top left is the Ca II K-H index vs the Ca II HK-K index, the top right is the Ca II K-H index vs the Ca II HK-H index, the center is the Ca II HK-K index vs the Ca II HK-H index, the bottom left is the Ca II K-H index vs the Hδ index, and the bottom right is the Ca II K-H index vs the Hγ index.

Chapter 4

Conclusions

We wanted to see if the Ca II H and K lines could be used to form a temperature index. These lines are present in very cool stars, and the Ca II H line is a blend with the Hϵ line in hotter stars, so it seemed like a temperature index involving these two lines should cover a broader range of spectral types than many existing temperature indices. Additionally, since these two lines are so close in wavelength, an index based on these lines should be relatively reddening free.

The Ca II K-H index appears to be the best index that we examined, specifically the form of the index with non-continuum calibrated spectra and Gaussian filters. It has the widest range in magnitude, which allows for greater precision. It also appears to cover a very wide range of spectral types. We did find a definite correlation between the index values and temperature, and it does not appear to be affected by metal content. There is definitely a strong correlation between spectral type and the Ca II K-H index for stars of spectral type lower than A0. We do see a correlation in the hotter stars and in the plots of index values vs temperature, but the errors are higher, most likely because we have fewer data points in those cases. For future research, it would be very useful to obtain spectra on more stars with spectral type hotter than A0, and more stars with known temperatures.

We also found that the Hδ and Hγ indices are good temperature indices that should be studied further. These indices are at least as good as the Hβ index. The Hδ index in particular has a lot of potential as a photometric temperature index, since the Strömgren v filter has a central wavelength very close to Hδ and could be used for Hδ photometry along with a narrower Hδ filter.

The motivation behind this project was to investigate the use of these lines as a temperature index with the idea of eventually constructing narrow-band photometric

filters based on the Ca II H and K lines. We have shown that the Ca II K-H index can be used as a temperature indicator. With its wide magnitude range, it should be possible to obtain temperature and spectral type measurements with a high level of precision for a range of spectral types from early B to late K. The fact that the non-continuum calibrated spectra and Gaussian filters produced the best results is promising for photometric work, because the light we observe from stars has obviously not been continuum calibrated, and real filter functions tend to be much closer in shape to Gaussian than to square functions. The Ca II K-H index has the potential to be a very useful temperature indicator, and further investigation into its use as a photometric index should yield positive results.

Appendix A

Observations

Table A.1 lists previously published values from SIMBAD of spectral type, magnitude, temperature, [Fe/H], Hβ color index, and b-y color index for the 95 stars in our data set. Table A.2 lists average values of our new indices for wavelength calibrated spectra and Gaussian filters. Table A.3 lists average index values for wavelength calibrated spectra and square filters. Table A.4 lists average index values for continuum calibrated spectra and Gaussian filters. Table A.5 lists average index values for continuum calibrated spectra and square filters.

Table A.1: Previously published data for stars observed in this study

Star	Spectral Type	V Magnitude	Temperature (Kelvin)	[Fe/H]	Hβ	b-y
10 Tau	F9 IV-V	4.28	5981	-0.11	2.615	0.367
15 CVn	B7 III	6.28	–	–	2.712	-0.41
20 Vul	B7 Ve	5.903	–	–	2.632	-0.32
34 Her	A3 V	6.106	–	–	2.863	0.007
α Aql	A7 V	0.77	–	–	2.81	0.137
α Boo	K1.5 III	-0.04	4300	-0.47	–	0.753
α Cas	K0 IIIa	2.252	4610	-0.09	–	0.753
α Lyr	A0 V	0.03	9450	-0.55	2.903	0.003
α Sge	G1 II	4.392	5440	-0.15	2.591	0.492
AN Lyn	A7 IV-V	10.86	–	–	2.762	0.202
β Cas	F2 IV	2.27	–	–	2.709	0.216
β Gem	K0 IIIb	1.15	4865	-0.04	–	0.611
β Leo	A3 V	2.14	–	–	2.899	0.043
β Vir	F9 V	3.61	6176	0.13	2.628	0.354
b Her	F7 V	5.068	5868	-0.62	2.611	0.356
BX Cnc	A7 V	7.97	–	–	2.812	0.12
CL Dra	F0 IV	4.967	–	–	2.761	0.178
CN Dra	F0 III	6.339	–	–	–	0.19
CQ Lyn	F0	7.97	–	–	2.711	0.247
δ Del	A7 IIIp	4.434	7100	-0.2	2.738	0.191
DQ Cep	F1 IV	7.26	–	–	2.739	0.204
DX Cet	A5	7	–	–	2.746	0.189
EO UMa	A7 III	7.126	–	–	–	0.181
ϵ Cep	F0 IV	4.19	–	–	2.761	0.171
η Cas	G0 V	3.45	5946	-0.31	2.588	0.372
FP Ser	A7 Vn	6.287	–	–	2.834	0.101
γ Cnc	A1 IV	4.668	–	–	2.911	0
GJ635b	G7 V	5.556	–	–	–	–

Continued on Next Page...

Table A.1 – Continued

Star	Spectral Type	V Magnitude	Temperature (Kelvin)	[Fe/H]	Hβ	b-y
GN And	A7 III	5.219	7270	-0.2	2.754	0.169
GW UMa	F3 V	9.67	–	–	–	–
GX Peg	A5m	6.34	–	–	2.821	0.118
HD 107655	A0 V	6.176	–	–	2.893	-0.005
HD 115612	B9.5 V	6.194	–	–	2.833	-0.025
HD 117043	G6 V	6.5	–	–	–	0.458
HD 127304	A0 Vs	6.055	–	–	2.879	-0.01
HD 158148	B5 V	5.51	–	–	2.688	-0.04
HD 158633	K0 V	6.43	–	–	2.55	0.463
HD 182572	G8 IV	5.16	5380	0.15	–	–
HD 184499	G0 V	6.61	5711	-0.61	2.578	0.39
HD 186791	K3 II	2.724	4210	-0.29	–	0.936
HD 187691	F8 V	5.1	6146	0.09	2.624	0.357
HD 192043	B8 III	7.6	–	–	–	–
HR 226	B5 V	4.524	6072	0.06	2.71	-0.72
HR 3799	A2 V	4.479	–	–	2.877	0.022
HR 3881	G0.5 Va	5.1	5899	–	2.612	0.389
HR 4112	F8 V	4.831	6072	-0.23	2.618	0.341
HR 4141	F1 V	5.161	–	–	2.716	0.228
HR 4227	A2 V	5.314	–	–	2.86	0.024
HR 4496	G8 V	5.32	5538	0.03	2.571	0.444
HR 4564	A3 V	5.531	8542	0.37	2.87	0.067
HR 4943	B9 V	5.191	–	–	2.819	-0.023
HR 5405	F0m	5.406	7754	0.1	2.817	0.123
HR 5468	A1 V	5.395	–	–	2.91	0.00
HR 5691	F9 IV	5.1	6172	-0.02	2.628	0.354
HR 5739	M1 III	5.167	–	–	–	–
HR 5901	K1 Iva	4.82	4800	-0.04	–	0.615
HR 6458	G0 V	5.4	5676	-0.41	2.59	0.404
HR 6623	G5 IV	3.41	5520	0.04	2.614	0.468
HR 6688	K2 III	3.741	4420	-0.09	–	–
HR 6705	K5 III	2.23	3930	-0.14	–	0.941
HR 6850	F5 V	5.03	6587	-0.31	2.653	0.281
HR 7061	F6 V	4.2	6369	-0.11	2.652	0.314
HR 7141	A5 V	4.62	–	–	2.856	0.084
HR 7420	A5 Vn	3.769	–	–	2.833	0.08
HR 7834	F5 Iab	4.016	6526	0.21	2.695	0.257
HR 8266	A5 V	5.052	–	–	2.82	0.122
HR 8622	09 V	4.877	–	–	2.588	-0.067
HR 8665	F7 V	4.2	6228	-0.32	2.626	0.331
HR 8969	F7 V	4.13	6255	-0.17	2.625	0.33
HR 9072	F4 IV	4.036	6576	-0.27	2.668	0.268
HT Peg	A4 Vn	5.314	–	–	2.836	0.099
ι Oph	B8 V	4.38	–	–	2.776	-0.039
ι Psc	F7 V	4.13	6255	-0.17	2.625	0.33
IP UMa	A5	7.66	–	–	2.783	0.178
NSV 6899	A4 V	5.918	–	–	2.868	0.064
ω Dra	F5 V	4.8	6720	0.4	–	0.289
SAO 88295	A3 III	5.519	–	–	2.895	0.045
σ Her	B9 V	4.2	–	–	2.791	0.006
τ Boo	F6 IV	4.5	6462	0	2.656	0.318
τ Cyg	F0 IV	3.72	–	–	2.684	0.255
τ Peg	A5 V	4.592	–	–	2.808	0.105
V340 And	A1 III	5.564	–	–	2.878	0.056
V350 Peg	F2	7.19	–	–	–	0.229

Continued on Next Page...

Table A.1 – Continued

Star	Spectral Type	V Magnitude	Temperature (Kelvin)	[Fe/H]	Hβ	b-y
V377 Cas	F0	7.83	–	–	2.679	0.212
V388 Cep	F0 IV	5.553	–	–	–	–
V549 Lyr	A3	8.07	–	–	2.814	0.129
V554 Lyr	B9	8.1	–	–	–	–
V873 Her	F0	8.4	–	–	2.746	0.23
V966 Her	F2	7.98	–	–	–	0.204
V1003 Her	A7	9.83	–	–	–	–
V1438 Aql	F0	7.72	–	–	2.726	0.28
V1624 Cyg	B2.5 Ve	4.929	–	–	2.553	–
V2109 Cyg	F0	7.52	–	–	–	0.202
x Her	A4 V	5.836	–	–	2.849	0.072
XX Psc	F0 Vn	6.118	–	–	2.773	0.165

Table A.2: Average Index Values - Wavelength Calibrated Spectra, Gaussian Filters

Star	Ca II K-H	Ca II HK-K	Ca II HK-H	Hδ	Hγ	Ca II (K-H) - Hδ	Ca II (K-H) - Hγ
10 Tau	-0.0404	–	–	0.884	1.667	-0.924	-1.707
15 CVn	-0.493	-0.980	-1.473	1.428	1.437	-1.922	-1.930
20 Vul	-0.407	-1.040	-1.447	1.412	1.386	-1.818	-1.793
34 Her	-0.636	-0.986	-1.622	1.572	1.569	-2.208	-2.205
α Aql	-0.401	-1.133	-1.534	1.493	1.483	-1.893	-1.884
α Boo	0.848	–	–	1.301	1.270	-0.452	-0.421
α Cas	0.070	–	–	1.147	1.139	-1.07665	-1.069
α Lyr	-0.759	-1.048	-1.807	1.650	1.611	-2.407	-2.370
α Sge	-0.115	-1.273	-1.388	1.206	1.195	-1.321	-1.310
AN Lyn	–	–	–	1.184	1.141	–	–
β Cas	-0.084	–	–	1.388	1.392	-1.472	-1.475
β Gem	-0.0510	-0.872	-0.923	1.169	1.155	-1.220	-1.206
β Leo	-0.623	-1.003	-1.626	1.609	1.597	-2.232	-2.220
β Vir	0.0762	-1.797	-1.721	1.282	1.266	-1.206	-1.190
b Her	-0.0594	-1.349	-1.408	1.289	1.270	-1.348	-1.329
BX Cnc	-0.354	-1.077	-1.431	1.477	1.549	-1.831	-1.903
CL Dra	-0.338	-1.156	-1.493	1.447	1.462	-1.785	-1.800
CN Dra	-0.274	-1.196	-1.470	1.430	1.466	-1.704	-1.740
CQ Lyn	-0.276	–	–	1.334	1.441	-1.609	-1.717
δ Del	-0.354	–	–	1.434	1.419	-1.788	-1.772
DQ Cep	-0.151	-1.303	-1.455	1.411	1.444	-1.562	-1.595
DX Cet	-0.298	-1.153	-1.451	1.448	1.490	-1.747	-1.788
EO UMa	-0.282	-1.112	-1.394	1.423	1.439	-1.705	-1.721
ϵ Cep	-0.351	–	–	1.449	1.426	-1.800	-1.777
η Cas	0.0963	–	–	1.262	1.225	-1.165	-1.129
FP Ser	-0.432	-1.043	-1.476	1.539	1.514	-1.972	-1.946
γ Cnc	-0.815	-0.879	-1.694	1.629	1.620	-2.444	-2.435
GJ635b	0.0887	-1.512	-1.423	1.252	1.218	-1.163	-1.130
GN And	-0.309	-0.651	-0.960	1.450	1.436	-1.758	-1.745
GW UMa	–	–	–	1.425	1.468	-1.425	-1.468
GX Peg	-0.446	-1.096	-1.543	1.519	1.510	-1.965	-1.957
HD 107655	-0.795	-0.890	-1.685	1.628	1.641	-2.424	-2.437
HD 115612	-0.753	-0.891	-1.644	1.578	1.589	-2.331	-2.343

Continued on Next Page...

Table A.2 – Continued

Star	Ca II K-H	Ca II HK-K	Ca II HK-H	Hδ	Hγ	Ca II (K-H) - Hδ	Ca II (K-H) - Hγ
HD 117043	0.172	-1.586	-1.414	1.211	1.185	-1.039	-1.013
HD 127304	-0.778	-0.893	-1.670	1.614	1.625	-2.392	-2.403
HD 158148	-0.472	-0.992	-1.464	1.412	1.4258	-1.884	-1.898
HD 158633	-0.0153	-1.375	-1.391	1.192	1.160	-1.207	-1.175
HD 182572	-0.0424	-1.335	-1.377	1.220	1.168	-1.262	-1.211
HD 184499	-0.0953	-1.275	-1.371	1.262	1.252	-1.358	-1.347
HD 186791	0.174	-1.620	-1.447	1.139	1.148	-0.956	-0.975
HD 187691	-0.0918	-0.546	-0.638	1.284	1.269	-1.376	-1.360
HD 192043	-0.456	-0.997	-1.454	1.448	1.499	-1.905	-1.955
HR 226	-0.447	-1.020	-1.467	1.433	1.419	-1.880	-1.866
HR 3799	-0.739	-0.929	-1.669	1.613	1.598	-2.353	-2.338
HR 3881	0.0699	-1.503	-1.433	1.263	1.238	-1.193	-1.168
HR 4112	0.0008	-1.409	-1.408	1.286	1.278	-1.285	-1.277
HR 4141	-0.214	-1.229	-1.443	1.387	1.411	-1.601	-1.624
HR 4227	-0.650	-0.975	-1.625	1.596	1.599	-2.246	-2.249
HR 4496	0.103	-1.490	-1.387	1.214	1.186	-1.111	-1.083
HR 4564	-0.673	-0.974	-1.647	1.586	1.572	-2.258	-2.245
HR 4943	-0.695	-0.920	-1.614	1.555	1.551	-2.250	-2.246
HR 5405	-0.464	-1.079	-1.543	1.479	1.511	-1.944	-1.975
HR 5468	-0.829	-0.876	-1.706	1.647	1.634	-2.476	-2.463
HR 5691	0.00967	-1.429	-1.420	1.292	1.278	-1.282	-1.268
HR 5739	0.376	-1.815	-1.440	1.171	1.171	-0.795	-0.796
HR 5901	0.211	-1.643	-1.432	1.181	1.149	-0.970	-0.938
HR 6458	0.0770	-1.500	-1.423	1.247	1.209	-1.170	-1.132
HR 6623	0.123	-1.544	-1.421	1.227	1.188	-1.103	-1.065
HR 6688	0.233	-1.696	-1.462	1.168	1.138	-0.935	-0.904
HR 6705	0.258	-1.727	-1.469	1.162	1.151	-0.904	-0.893
HR 6850	-0.194	-1.182	-1.375	1.334	1.371	-1.528	-1.565
HR 7061	-0.0362	-1.379	-1.415	1.319	1.322	-1.355	-1.358
HR 7141	-0.516	-1.063	-1.579	1.556	1.560	-2.072	-2.076
HR 7420	-0.421	-1.145	-1.566	1.532	1.498	-1.953	-1.920
HR 7834	-0.0192	-1.466	-1.485	1.349	1.383	-1.368	-1.402
HR 8266	-0.435	-1.113	-1.547	1.510	1.494	-1.945	-1.929
HR 8622	-0.234	-1.090	-1.325	1.291	1.289	-1.526	-1.523
HR 8665	-0.0018	-1.408	-1.410	1.294	1.279	-1.296	-1.280
HR 8969	0.0496	-1.465	-1.415	1.295	1.276	-1.246	-1.227
HR 9072	-0.0945	-1.316	-1.410	1.341	1.360	-1.435	-1.454
HT Peg	-0.516	–	–	1.538	1.505	-2.054	-2.021
ι Oph	-0.611	-0.952	-1.563	1.503	1.503	-2.114	-2.114
ι Psc	0.0549	-1.464	-1.409	1.293	1.276	-1.239	-1.221
IP UMa	–	–	–	1.437	1.451	–	–
NSV 6899	-0.684	-0.976	-1.660	1.597	1.577	-2.812	-2.261
ω Dra	-0.213	-1.176	-1.389	1.342	1.404	-1.555	-1.617
SAO 88295	-0.626	–	–	1.593	1.557	-2.219	-2.183
σ Her	-0.631	-0.954	-1.586	1.525	1.526	-2.156	-2.157
τ Boo	-0.0269	-1.397	-1.424	1.317	1.319	-1.344	-1.346
τ Cyg	-0.111	-1.310	-1.420	1.357	1.363	-1.468	-1.474
τ Peg	-0.477	–	–	1.524	1.503	-2.001	-1.980
V340 And	-0.687	–	–	1.630	1.556	-2.316	-2.242
V350 Peg	-0.0549	–	–	1.394	1.394	-1.449	-1.449
V377 Cas	-0.0988	–	–	1.486	1.400	-1.585	-1.499
V388 Cep	-0.363	–	–	1.466	1.447	-1.829	-1.810
V549 Lyr	-0.295	–	–	1.585	1.472	-1.881	-1.767
V554 Lyr	-0.410	–	–	1.448	1.650	-1.858	-2.060
V873 Her	-0.295	–	–	1.389	1.932	-1.684	-2.227

Continued on Next Page...

Table A.2 – Continued

Star	Ca II K-H	Ca II HK-K	Ca II HK-H	Hδ	Hγ	Ca II (K-H) - Hδ	Ca II (K-H) - Hγ
V966 Her	-0.199	-1.206	-1.405	1.414	1.459	-1.613	-1.658
V1003 Her	–	–	–	1.338	1.895	–	–
V1438 Aql	-0.213	-0.641	-0.854	1.413	1.505	-1.625	-1.718
V1624 Cyg	-0.290	-1.079	-1.369	1.330	1.321	-1.620	-1.611
V2109 Cyg	-0.229	-1.169	-1.398	1.396	1.451	-1.625	-1.680
x Her	-0.650	-0.978	-1.628	1.567	1.564	-2.217	-2.214
XX Psc	-0.338	–	–	1.477	1.451	-1.815	-1.789

Table A.3: Average Index Values - Wavelength Calibrated Spectra, Square Filters

Star	Ca II K-H	Ca II HK-K	Ca II HK-H	Hδ	Hγ	Ca II (K-H) - Hδ	Ca II (K-H) - Hγ
10 Tau	0.105	–	–	1.405	0.914	-1.300	-2.384
15 CVn	-0.413	-1.010	-1.424	1.390	1.404	-1.803	-3.335
20 Vul	-0.323	-1.074	-1.397	1.375	1.361	-1.698	-3.153
34 Her	-0.562	-1.002	-1.564	1.553	1.554	-2.114	-3.759
α Aql	-0.356	-1.123	-1.478	1.468	1.463	-1.824	-3.346
α Cas	0.127	–	–	1.010	1.071	-0.973	-2.139
α Lyr	-0.640	-1.114	-1.754	1.614	1.580	-2.253	-3.951
α Sge	-0.0907	-1.237	-1.328	1.179	1.142	-1.270	-2.452
AN Lyn	–	–	–	1.124	1.108	–	–
β Cas	-0.0361	–	–	1.359	1.354	-1.395	-2.830
β Gem	0.0536	-0.888	-0.0834	1.116	1.140	-1.062	-2.346
β Leo	-0.545	-1.028	-1.573	1.593	1.588	-2.138	-3.808
β Vir	0.160	-1.835	-1.675	1.245	1.245	-1.084	-2.435
b Her	-0.0629	-1.260	-1.323	1.260	1.239	-1.322	-2.568
BX Cnc	-0.274	-1.144	-1.417	1.454	1.533	-1.727	-3.437
CL Dra	-0.313	-1.117	-1.430	1.419	1.440	-1.732	-3.240
CN Dra	-0.251	-1.158	-1.410	1.400	1.441	-1.651	-3.181
CQ Lyn	-0.209	–	–	1.309	1.418	-1.518	-3.135
δ Del	-0.309	–	–	1.409	1.383	-1.718	-3.156
DQ Cep	-0.146	-1.238	-1.384	1.376	1.411	-1.523	-3.006
DX Cet	-0.274	-1.129	-1.403	1.418	1.463	-1.692	-3.251
EO UMa	-0.193	-1.191	-1.384	1.392	1.425	-1.585	-3.146
ϵ Cep	-0.304	–	–	1.422	1.393	-1.726	-3.170
η Cas	0.127	–	–	1.228	1.180	-1.101	-2.309
FP Ser	-0.326	-1.160	-1.486	1.512	1.500	-1.838	-3.446
γ Cnc	-0.704	-0.931	-1.635	1.603	1.602	-2.308	-4.036
GJ 635b	0.0862	-1.41	-1.324	1.212	1.168	-1.126	-2.298
GN And	0.00661	-0.637	-0.631	1.420	1.405	-1.414	-3.150
GW UMa	–	–	–	1.404	1.433	–	–
GX Peg	-0.400	-1.095	-1.495	1.491	1.474	-1.891	-3.430
HD 107655	-0.679	-0.944	-1.623	1.594	1.614	-2.273	-4.050
HD 115612	-0.635	-0.943	-1.578	1.532	1.551	-2.168	-3.894
HD 117043	0.197	-1.494	-1.297	1.163	1.149	-0.966	-2.162
HD 127304	-0.656	-0.947	-1.604	1.571	1.587	-2.227	-3.990
HD 158148	-0.391	-1.023	-1.414	1.374	1.395	-1.765	-3.293
HD 158633	0.0134	-1.329	-1.316	1.146	1.120	-1.133	-2.295
HD 182572	-0.0123	-1.303	-1.315	1.164	1.100	-1.176	-2.231
HD 184499	-0.0925	-1.225	-1.317	1.231	1.186	-1.324	-2.533

Continued on Next Page...

Table A.3 – Continued

Star	Ca II K-H	Ca II HK-K	Ca II HK-H	Hδ	Hγ	Ca II (K-H) - Hδ	Ca II (K-H) - Hγ
HD 186791	0.230	-1.612	-1.382	1.076	1.112	-0.847	-2.086
HD 187691	-0.0740	-1.258	-1.332	1.247	1.225	-1.321	-2.585
HD 192043	-0.383	-1.030	-1.413	1.407	1.456	-1.790	-3.412
HR 226	-0.364	-1.059	-1.422	1.395	1.382	-1.758	-3.248
HR 3799	-0.637	-0.967	-1.604	1.584	1.575	-2.221	-3.913
HR 3881	0.0712	-1.398	-1.327	1.229	1.211	-1.158	-2.378
HR 4112	0.00117	-1.321	-1.319	1.256	1.251	-1.254	-2.528
HR 4141	-0.203	-1.173	-1.376	1.360	1.391	-1.563	-3.015
HR 4227	-0.546	-1.013	-1.560	1.560	1.571	-2.106	-3.820
HR 4496	0.124	-1.424	-1.301	1.169	1.158	-1.045	-2.241
HR 4564	-0.586	-0.995	-1.581	1.556	1.553	-2.142	-3.798
HR 4943	-0.577	-0.968	-1.545	1.509	1.511	-2.086	-3.757
HR 5405	-0.422	-1.060	-1.481	1.449	1.485	-1.871	-3.460
HR 5468	-0.713	-0.936	-1.649	1.624	1.619	-2.337	-4.083
HR 5691	-0.0001	-1.327	-1.328	1.259	1.240	-1.260	-2.509
HR 5739	0.356	-1.716	-1.360	1.107	1.135	-0.751	-1.931
HR 5901	0.244	-1.567	-1.324	1.125	1.115	-0.881	-2.053
HR 6458	0.0687	-1.396	-1.328	1.208	1.162	-1.139	-2.294
HR 6623	0.136	-1.455	-1.319	1.178	1.149	-1.042	-2.213
HR 6688	0.274	-1.622	-1.348	1.103	1.101	-0.829	-2.005
HR 6705	0.292	-1.679	-1.387	1.090	1.113	-0.799	-2.006
HR 6850	-0.187	-1.142	-1.329	1.304	1.318	-1.492	-2.883
HR 7061	-0.0384	-1.292	-1.331	1.291	1.296	-1.329	-2.655
HR 7141	-0.452	-1.068	-1.520	1.532	1.541	-1.984	-3.617
HR 7420	-0.350	-1.151	-1.500	1.505	1.470	-1.854	-3.390
HR 7834	-0.0349	-1.340	-1.375	1.313	1.349	-1.348	-2.751
HR 8266	-0.386	-1.105	-1.491	1.485	1.469	-1.871	-3.398
HR 8622	-0.194	-1.107	-1.301	1.277	1.266	-1.471	-2.789
HR 8665	-0.00683	-1.320	-1.326	1.264	1.241	-1.271	-2.522
HR 8969	0.0435	-1.372	-1.329	1.263	1.241	-1.220	-2.468
HR 9072	-0.0910	-1.248	-1.339	1.311	1.328	-1.402	-2.782
HT Peg	-0.447	–	–	1.517	1.486	-1.964	-3.507
ι Oph	-0.500	-0.998	-1.499	1.458	1.464	-1.958	-3.578
ι Psc	0.384	-1.684	-1.299	1.260	1.242	-0.876	-2.463
IP UMa	–	–	–	1.409	1.426	–	–
NSV 6899	-0.598	-0.997	-1.595	1.572	1.559	-2.169	-3.820
ω Dra	-0.201	-1.144	-1.345	1.309	1.354	-1.510	-2.971
SAO 88295	-0.555	–	–	1.564	1.533	-2.119	-3.716
σ Her	-0.529	-0.989	-1.518	1.478	1.486	-2.007	-3.643
τ Boo	-0.0299	-1.305	-1.335	1.284	1.291	-1.314	-2.637
τ Cyg	-0.109	-1.245	-1.354	1.327	1.328	-1.436	-2.802
τ Peg	-0.416	–	–	1.501	1.479	-1.917	-3.458
V340 And	-0.603	–	–	1.608	1.535	-2.211	-3.777
V350 Peg	-0.00263	–	–	1.364	1.345	-1.366	-2.793
V377 Cas	-0.00925	–	–	1.452	1.366	-1.461	-2.865
V388 Cep	-0.310	–	–	1.438	1.412	-1.748	-3.222
V549 Lyr	-0.194	–	–	1.552	1.444	-1.745	-3.211
V554 Lyr	-0.384	–	–	1.427	1.581	-1.811	-3.641
V873 Her	-0.214	–	–	1.360	1.660	-1.573	-3.887
V966 Her	-0.125	-1.249	-1.374	1.384	1.435	-1.509	-3.094
V1003 Her	–	–	–	1.329	1.792	–	–
V1438 Aql	-0.208	-0.592	-0.800	1.382	1.459	-1.590	-3.177
V1624 Cyg	-0.236	-1.098	-1.334	1.304	1.310	-1.540	-2.921
V2109 Cyg	-0.215	-1.141	-1.356	1.374	1.418	-1.589	-3.097
x Her	-0.571	-0.993	-1.564	1.536	1.538	-2.106	-3.752

Continued on Next Page...

Table A.3 – Continued

Star	Ca II K-H	Ca II HK-K	Ca II HK-H	Hδ	Hγ	Ca II (K-H) - Hδ	Ca II (K-H) - Hγ
XX Psc	-0.272	–	–	1.448	1.423	-1.720	-3.212

Table A.4: Average Index Values - Continuum Calibrated Spectra, Gaussian Filters

Star	Ca II K-H	Ca II HK-K	Ca II HK-H	Hδ	Hγ	Ca II (K-H) - Hδ	Ca II (K-H) - Hγ
10 Tau	-0.0269	–	–	1.269	1.241	-1.296	-1.268
15 CVn	-0.356	-1.075	-1.431	1.425	1.439	-1.780	-1.798
20 Vul	-0.327	-1.091	-1.418	1.409	1.406	-1.736	-1.733
34 Her	-0.544	-1.049	-1.593	1.571	1.570	-2.115	-2.114
α Aql	-0.352	-1.169	-1.521	1.491	1.481	-1.844	-1.833
α Cas	0.000403	–	–	1.148	1.133	-1.148	-1.133
α Lyr	-0.689	-0.947	-1.636	1.648	1.610	-2.337	-2.299
α Sge	0.0209	-1.379	-1.358	1.203	1.183	-1.182	-1.162
AN Lyn	–	–	–	1.181	1.138	–	–
β Cas	-0.126	–	–	1.389	1.390	-1.515	-1.516
β Gem	-0.124	-1.560	-1.684	1.170	1.153	-1.294	-1.277
β Leo	-0.575	-1.037	-1.612	1.609	1.595	-2.184	-2.170
β Vir	0.0527	-1.574	-1.522	1.283	1.269	-1.230	-1.216
b Vir	0.0498	-1.432	-1.383	1.287	1.272	-1.238	-1.223
BX Cnc	-0.275	-1.134	-1.409	1.476	1.548	-1.751	-1.823
CL Dra	-0.227	-1.236	-1.463	1.445	1.463	-1.673	-1.690
CN Dra	-0.182	-1.264	-1.446	1.488	1.468	-1.671	-1.650
CQ Lyn	-0.111	–	–	1.332	1.439	-1.442	-1.550
δ Del	-0.246	–	–	1.432	1.419	-1.678	-1.665
DQ Cep	-0.102	-1.340	-1.442	1.410	1.445	-1.512	-1.547
DX Cet	-0.187	-1.235	-1.422	1.445	1.491	-1.632	-1.678
EO UMa	-0.211	-1.164	-1.375	1.422	1.439	-1.633	-1.650
ϵ Cep	-0.261	–	–	1.447	1.425	-1.708	-1.686
η Cas	0.0651	–	–	1.262	1.222	-1.197	-1.157
FP Ser	-0.363	-1.094	-1.457	1.538	1.514	-1.902	-1.877
γ Cnc	-0.684	-0.966	-1.650	1.626	1.617	-2.310	-2.301
GJ 635b	0.150	-1.562	-1.411	1.252	1.219	-1.102	-1.068
GN And	-0.257	-1.121	-1.379	1.450	1.439	-1.707	-1.696
GW UMa	–	–	–	1.422	1.467	–	–
GX Peg	-0.362	-1.156	-1.519	1.515	1.507	-1.877	-1.870
HD 107655	-0.683	-0.965	-1.648	1.626	1.642	-2.308	-2.325
HD 115612	-0.614	-0.984	-1.598	1.574	1.592	-2.188	-2.207
HD 117043	0.163	-1.580	-1.417	1.213	1.180	-1.050	-1.017
HD 127304	-0.661	-0.970	-1.631	1.611	1.627	-2.273	-2.289
HD 158148	-0.360	-1.069	-1.429	1.409	1.427	-1.769	-1.787
HD 158633	0.110	-1.474	-1.364	1.191	1.161	-1.081	-1.051
HD 182572	0.00569	-1.373	-1.367	1.221	1.182	-1.215	-1.176
HD 184499	0.0109	-1.355	-1.344	1.260	1.239	-1.249	-1.228
HD 186791	0.134	-1.585	-1.451	1.140	1.144	-1.006	-1.011
HD 187691	0.0246	-1.388	-1.364	1.280	1.263	-1.255	-1.238
HD 192043	-0.319	-1.093	-1.413	1.443	1.497	-1.762	-1.817
HR 226	-0.334	-1.010	-1.434	1.427	1.418	-1.761	-1.752
HR 3799	-0.630	-1.004	-1.634	1.611	1.596	-2.241	-2.226
HR 3881	0.140	-1.561	-1.420	1.264	1.237	-1.123	-1.097

Continued on Next Page...

Table A.4 – Continued

Star	Ca II K-H	Ca II HK-K	Ca II HK-H	Hδ	Hγ	Ca II (K-H) - Hδ	Ca II (K-H) - Hγ
HR 4112	0.0952	-1.483	-1.388	1.285	1.281	-1.190	-1.185
HR 4141	-0.108	-1.308	-1.416	1.386	1.411	-1.493	-1.517
HR 4227	-0.591	-1.016	-1.607	1.596	1.596	-2.186	-2.187
HR 4496	0.180	-1.558	-1.378	1.215	1.184	-1.035	-1.004
HR 4564	-0.575	-1.041	-1.616	1.584	1.571	-2.159	-2.145
HR 4943	-0.562	-1.009	-1.571	1.551	1.551	-2.113	-2.113
HR 5405	-0.355	-1.157	-1.512	1.477	1.510	-1.832	-1.866
HR 5468	-0.714	-0.952	-1.667	1.643	1.633	-2.357	-2.347
HR 5691	0.106	-1.506	-1.399	1.291	1.280	-1.184	-1.173
HR 5739	0.354	-1.785	-1.431	1.170	1.170	-0.816	-0.816
HR 5901	0.191	-1.628	-1.437	1.182	1.143	-0.991	-0.953
HR 6458	0.135	-1.546	-1.411	1.247	1.211	-1.112	-1.076
HR 6623	0.164	-1.578	-1.415	1.227	1.185	-1.064	-1.021
HR 6688	0.198	-1.668	-1.470	1.168	1.133	-0.970	-0.935
HR 6705	0.186	-1.666	-1.480	1.163	1.146	-0.976	-0.960
HR 6850	-0.0311	-1.302	-1.334	1.327	1.361	-1.358	-1.392
HR 7061	0.0412	-1.439	-1.398	1.319	1.323	-1.277	-1.282
HR 7141	-0.471	-1.095	-1.566	1.557	1.563	-2.028	-2.034
HR 7420	-0.448	-1.126	-1.574	1.531	1.493	-1.979	-1.941
HR 7834	0.0672	-1.535	-1.468	1.348	1.389	-1.280	-1.322
HR 8266	-0.363	-1.165	-1.528	1.507	1.492	-1.871	-1.856
HR 8622	-0.116	-1.176	-1.292	1.287	1.288	-1.404	-1.405
HR 8665	0.0778	-1.471	-1.393	1.292	1.277	-1.215	-1.199
HR 8969	0.0993	-1.505	-1.405	1.295	1.275	-1.195	-1.176
HR 9072	-0.0157	-1.376	-1.391	1.340	1.364	-1.355	-1.379
HT Peg	-0.453	–	–	1.537	1.505	-1.990	-1.958
ι Oph	-0.517	-1.016	-1.533	1.501	1.504	-2.018	-2.021
ι Psc	0.113	-1.504	-1.391	1.294	1.286	-1.181	-1.173
IP UMa	–	–	–	1.434	1.450	–	–
NSV 6899	-0.597	-1.036	-1.632	1.596	1.578	-2.193	-2.175
ω Dra	-0.0330	-1.310	-1.343	1.335	1.397	-1.368	-1.430
SAO 88295	-0.514	–	–	1.590	1.554	-2.104	-2.069
σ Her	-0.505	-1.040	-1.546	1.522	1.527	-2.027	-2.033
τ Boo	0.0710	-1.474	-1.403	1.316	1.321	-1.245	-1.250
τ Cyg	-0.0258	-1.375	-1.400	1.355	1.363	-1.380	-1.388
τ Peg	-0.398	–	–	1.523	1.501	-1.922	-1.899
V340 And	-0.592	–	–	1.627	1.555	-2.219	-2.147
V350 Peg	-0.0978	–	–	1.394	1.391	-1.492	-1.490
V377 Cas	-0.164	–	–	1.488	1.400	-1.652	-1.563
V388 Cep	-0.270	–	–	1.465	1.445	-1.734	-1.715
V549 Lyr	-0.293	–	–	1.585	1.464	-1.878	-1.757
V554 Lyr	-0.226	–	–	1.442	1.645	-1.668	-1.870
V873 Her	-0.147	–	–	1.385	1.925	-1.532	-2.073
V966 Her	-0.171	-1.213	-1.384	1.411	1.463	-1.583	-1.634
V1003 Her	–	–	–	1.331	1.869	–	–
V1438 Aql	-0.115	-1.272	-1.387	1.409	1.502	-1.524	-1.617
V1624 Cyg	-0.191	-1.150	-1.341	1.327	1.322	-1.518	-1.513
V2109 Cyg	-0.0626	-1.293	-1.356	1.390	1.449	-1.452	-1.512
x Her	-0.537	-1.055	-1.592	1.565	1.564	-2.102	-2.100
XX Psc	-0.316	–	–	1.477	1.449	-1.794	-1.766

Table A.5: Average Index Values - Continuum Calibrated Spectra, Square Filters

Star	Ca II K-H	Ca II HK-K	Ca II HK-H	Hδ	Hγ	Ca II (K-H) - Hδ	Ca II (K-H) - Hγ
10 Tau	0.0209	–	–	1.238	1.194	-1.216	-1.173
15 CVn	-0.276	-1.104	-1.380	1.384	1.408	-1.660	-1.683
20 Vul	-0.247	-1.124	-1.372	1.371	1.376	-1.619	-1.624
34 Her	-0.470	-1.065	-1.535	1.551	1.555	-2.021	-2.024
α Aql	-0.307	-1.160	-1.466	1.467	1.460	1.774	-1.767
α Cas	0.0537	–	–	1.102	1.062	-1.048	-1.009
α Lyr	-0.569	-1.014	-1.583	1.611	1.578	-2.181	-2.148
α Sge	0.0455	-1.436	-1.300	1.174	1.125	-1.128	-1.080
AN Lyn	–	–	–	1.119	1.104	–	–
β Cas	-0.0766	–	–	1.360	1.352	-1.437	-1.429
β Gem	-0.0151	-1.572	-1.587	1.117	1.136	-1.132	-1.151
β Leo	-0.497	-1.063	-1.560	1.593	1.584	-2.090	-2.082
β Vir	0.137	-1.167	-1.030	1.245	1.249	-1.108	-1.113
b Her	0.0464	-1.344	-1.298	1.257	1.242	-1.211	-1.196
BX Cnc	-0.195	-1.203	-1.397	1.453	1.531	-1.648	-1.726
CL Dra	-0.202	-1.198	-1.401	1.416	1.441	-1.619	-1.643
CN Dra	-0.159	-1.227	-1.386	1.396	1.443	-1.555	-1.603
CQ Lyn	-0.453	–	–	1.305	1.415	-1.351	-1.460
δ Del -0.201	–	–	1.405	1.383	-1.607	-1.585	
DQ Cep	-0.0969	-1.275	-1.372	1.375	1.413	-1.472	-1.510
DX Cet	-0.163	-1.212	-1.375	1.414	1.464	-1.576	-1.626
EO UMa	-0.123	-1.244	-1.367	1.391	1.424	-1.513	-1.547
ϵ Cep	-0.213	–	–	1.420	1.390	-1.633	-1.603
η Cas	0.0955	–	–	1.229	1.176	-1.133	-1.080
FP Ser	-0.257	-1.212	-1.469	1.511	1.499	-1.768	-1.757
γ Cnc	-0.573	-1.0195	-1.593	1.599	1.597	-2.172	-2.171
GJ 635b	0.148	-1.461	-1.314	1.213	1.169	-1.065	-1.021
GN And	-0.214	-1.112	-1.325	1.419	1.408	-1.633	-1.622
GW UMa	–	–	–	1.400	1.430	–	–
GX Peg	-0.315	-1.156	-1.471	1.485	1.470	-1.800	-1.785
HD 107655	-0.566	-1.019	-1.585	1.590	1.615	-2.156	-2.181
HD 115612	-0.496	-1.035	-1.531	1.527	1.556	-2.023	-2.052
HD 117043	0.188	-1.490	-1.302	1.166	1.140	-0.978	-0.952
HD 127304	-0.540	-1.024	-1.564	1.567	1.591	-2.107	-2.130
HD 158148	-0.279	-1.100	-1.378	1.370	1.398	-1.648	-1.676
HD 158633	0.139	-1.430	-1.291	1.145	1.121	-1.007	-0.983
HD 182572	0.0358	-1.343	-1.307	1.166	1.121	-1.130	-1.086
HD 184499	0.0137	-1.307	-1.293	1.228	1.167	-1.214	-1.153
HD 186791	0.190	-1.574	-1.384	1.077	1.107	-0.887	-0.917
HD 187691	0.0429	-1.349	-1.306	1.241	1.217	-1.198	-1.175
HD 192043	-0.246	-1.126	-1.371	1.400	1.455	-1.645	-1.700
HR 226	-0.251	-1.139	-1.390	1.387	1.380	-1.637	-1.631
HR 3799	-0.528	-1.042	-1.569	1.581	1.572	-2.109	-2.100
HR 3881	0.142	-1.457	-1.316	1.230	1.210	-1.088	-1.068
HR 4112	0.0957	-1.396	-1.301	1.255	1.254	-1.159	-1.158
HR 4141	-0.0968	-1.253	-1.349	1.358	1.392	-1.455	-1.488
HR 4227	-0.487	-1.055	-1.542	1.559	1.567	-2.046	-2.054
HR 4496	0.201	-1.492	-1.291	1.171	1.155	-0.970	-0.954
HR 4564	-0.488	-1.063	-1.551	1.554	1.550	-2.042	-2.038
HR 4943	-0.444	-1.058	-1.502	1.504	1.512	-1.948	-1.955
HR 5405	-0.312	-1.138	-1.450	1.445	1.484	-1.758	-1.796
HR 5468	-0.598	-1.013	-1.611	1.619	1.618	-2.217	-2.216
HR 5691	0.0970	-1.406	-1.309	1.258	1.243	-1.161	-1.146

Continued on Next Page...

Table A.5 – Continued

Star	Ca II K-H	Ca II HK-K	Ca II HK-H	Hδ	Hγ	Ca II (K-H) - Hδ	Ca II (K-H) - Hγ
HR 5739	0.335	-1.681	-1.346	1.105	1.133	-0.770	-0.798
HR 5901	0.224	-1.554	-1.330	1.126	1.107	-0.902	-0.883
HR 6458	0.127	-1.444	-1.317	1.208	1.165	-1.081	-1.038
HR 6623	0.176	-1.491	-1.315	1.179	1.144	-1.003	-0.968
HR 6688	0.239	-1.595	-1.356	1.104	1.094	-0.865	-0.855
HR 6705	0.220	-1.615	-2.396	1.091	1.106	-0.871	-0.887
HR 6850	-0.0248	-1.264	-1.289	1.295	1.303	-1.319	-1.328
HR 7061	0.0393	-1.354	-1.315	1.290	1.297	-1.251	-1.258
HR 7141	-0.407	-1.101	-1.508	1.533	1.545	-1.940	-1.952
HR 7420	-0.376	-1.134	-1.510	1.503	1.465	-1.880	-1.841
HR 7834	0.0517	-1.411	-1.359	1.311	1.357	-1.259	-1.305
HR 8266	-0.314	-1.158	-1.472	1.482	1.466	-1.796	-1.780
HR 8622	-0.0764	-1.192	-1.268	1.270	1.265	-1.347	-1.342
HR 8665	0.073	-1.384	-1.311	1.262	1.238	-1.189	-1.166
HR 8969	0.0934	-1.414	-1.321	1.262	1.239	-1.169	-1.146
HR 9072	-0.0118	-1.309	-1.321	1.309	1.333	-1.321	-1.345
HT Peg	-0.384	–	–	1.516	1.485	-1.900	-1.870
ι Oph	–	–	–	1.454	1.466	–	–
ι Psc	0.102	-1.408	-1.306	1.261	1.252	-1.159	-1.150
IP UMa	–	–	–	1.404	1.425	–	–
NSV 6899	-0.511	-1.057	-1.567	1.569	1.560	-2.080	-2.071
ω Dra	-0.0208	-1.280	-1.301	1.299	1.343	-1.320	-1.364
SAO 88295	-0.444	–	–	1.559	1.530	-2.003	-1.973
σ Her	-0.403	-1.073	-1.477	1.473	1.489	-1.876	-1.892
τ Boo	0.0684	-1.384	-1.315	1.283	1.293	-1.215	-1.224
τ Cyg	-0.0236	-1.311	-1.335	1.323	1.328	-1.347	-1.351
τ Peg	-0.338	–	–	1.499	1.476	-1.837	-1.814
V340 And	-0.509	–	–	1.605	1.532	-2.113	-2.041
V350 Peg	-0.0455	–	–	1.363	1.341	-1.409	-1.387
V377 Cas	-0.0739	–	–	1.454	1.366	-1.528	-1.440
V388 Cep	-0.217	–	–	1.435	1.410	-1.652	-1.627
V549 Lyr	-0.190	–	–	1.550	1.438	-1.739	-1.628
V554 Lyr	-0.199	–	–	1.420	1.573	-1.619	-1.772
V873 Her	-0.0670	–	–	1.354	1.653	-1.421	-1.720
V966 Her	-0.0926	-1.271	-1.364	1.380	1.439	-1.472	-1.531
V1003 Her	–	–	–	1.319	1.757	–	–
V1438 Aql	-0.110	-1.223	-1.333	1.377	1.454	-1.487	-1.565
V1624 Cyg	-0.137	-1.169	-1.306	1.300	1.311	-1.439	-1.448
V2109 Cyg	-0.0483	-1.266	-1.314	1.364	1.415	-1.412	-1.463
x Her	-0.458	-1.071	-1.528	1.533	1.537	-1.990	-1.994
XX Psc	-0.250	–	–	1.449	1.421	-1.699	-1.671

References

Anthony-Twarog, B. J., Laird, J. B., Payne, D., & Twarog, B. A. 1991, AJ, 101, 1902

Anthony-Twarog, B. J., Twarog, B., & Craig, J. 1995, PASP, 107, 32

Anthony-Twarog, B. J., & Twarog, B. J. 1998, AJ, 116, 1932

Beers, T. C., Preston, G. W., & Shectman, S. A. 1985, AJ, 90, 2089

Beers, T. C., Preston, G. W., Shectman, S. A., & Kage, J. A. 1990, AJ, 100, 849

Bohm-Vitense, E. 1989, "Introduction to Stellar Astrophysics" (Cambridge University Press)

Cardelli, J. A., Clayton, G. C., & Mathis, J. S. 1989, ApJ, 345, 245

Carroll, B. W. & Ostlie, D. A. 1996, "Modern Astrophysics" (Addison-Wesley Publishing Company, Inc.)

Chen, P. C., PASP, 94, 948

Crawford, D. L. & Mander, J. 1966 AJ, 7, 114

Freedman, R. A. & Kaufmann, W. J. III 2005, "Universe" 7E (W. H. Freeman and Company)

Hintz, M. L., Joner, M. D., & Hintz, E. G. 1998, AJ, 116, 2993

Kitchin, C. R. 1995, "Optical Astronomical Spectroscopy" (Institute of Physics Publishing)

Laverty, C. L. 2006, Senior Thesis, Brigham Young University

Linsky, J. L. & Avrett, E. H. 1970, PASP, 82, 169

Pasquini, L., de Medeiros, J. R., & Girardi, L. 2000, A&A, 361, 1011

Rose, M. B. 2006, Master's Thesis, Brigham Young University

SIMBAD database 2007, (http://simbad.u-strasbg.fr/simbad/)

Suntzeff, N. B., AJ, 85, 408

Tennyson, J. 2005, "Astronomical Spectroscopy" (Imperial College Press)

Twarog, B. A. & Anthony-Twarog, B. J. 1991, AJ, 101, 237

Twarog, B. A. & Anthony-Twarog, B. J. 1995, AJ, 109, 2828

Twarog, B. A., Anthony-Twarog, B. J., & Tanner, D. 2002, AJ, 123, 2715

Zelik, M. & Gregory, S. A. 1998, "Introductory Astronomy & Astrophysics" 4E (Saunders College Publishing)

Zinn, R. 1980, ApJ, 241, 602